

Technical University of Crete
School of Production Engineering and Management
Dynamic Systems and Simulation Laboratory



*Exploiting ACC Vehicles for improved traffic
flow on motorways*

Vandrou Foteini

Supervisor: Papageorgiou Markos

A thesis submitted in fulfillment of the requirements for the diploma of
Production Engineering and Management

Chania, 2018

The current Thesis by Vandorou Foteini is approved by the committee:

Professor Papageorgiou Markos, Supervisor

Associate Professor Papamichail Ioannis

Professor Nikolos Ioannis

Acknowledgements

Finilizing this thesis, I would like to thank my supervisor Prof. Markos Papageorgiou as well as Associate Prof. Ioannis Papamichail for the valueable help and guidance they provided me and also for giving me the opportunity to become a member of the Dynamic Systems and Simulation Laboratory (DSSL).

Furthermore, I would like to thank all the members of the DSSL for their assistance and support. Specifically, I would like to thank Dr. Diamantis Manolis and Dr. Anastasia Spiliopoulou for their collaboration and for the knowledge they offered me regarding this work.

Finally, I would like to thank my family for always being there for me and encouraging me, as well as my friends for all the fun we had throughout these years.

This thesis is dedicated to my father's memory.

Contents

Acknowledgements.....	3
List of Figures.....	6
List of Tables.....	8
Abstract.....	9
1. Introduction.....	10
1.1 Motivation.....	10
1.2 Thesis Objectives.....	12
1.3 Thesis Outline.....	12
2. Methodology.....	13
2.1 Traffic Control Concept.....	13
2.1.1 Capacity increase.....	15
2.1.2 Increase discharge flow.....	17
3. Application.....	20
3.1 Aimsun.....	20
3.2 Network description.....	21
3.3 IDM Model.....	23
3.4 Simulation Set-up.....	27
4. Simulation Investigations.....	30
4.1 No-Traffic Control Case.....	31
4.2 Traffic Control Case 1.....	33

4.2.1 Controller Settings	35
4.3 Traffic Control Case 2	39
4.4 Traffic Control Case 3	44
4.5 Traffic Control Case 4	47
4.6 Traffic Control Case 5	52
4.7 Traffic Control Cases Summary	57
5. Conclusions and Future Work.....	62
5.1 Thesis Summary.....	62
5.2 Conclusions.....	62
5.3 Future Work.....	63
References.....	64

List of Figures

Figure 1 : Illustration of the control system operation.....	14
Figure 2 : Single-lane fundamental diagram for various time-gaps.....	15
Figure 3 : Calculation of the suggested time-gap value using a linear function	16
Figure 4 : Calculation of the suggested time-gap value using a stepwise function	16
Figure 5 : Detection of the congestion head	18
Figure 6 : Conceptual Diagram of AIMSUN API	20
Figure 7 : Sketch of the Motorway A20 in The Netherlands	21
Figure 8 : (a) Spatio-temporal diagrams of real speed (b) Spatio-temporal diagrams of simulated speed .	22
Figure 9 : Real and simulated outflow from the merge area.....	23
Figure 10 : IDM Model in Stationary State	25
Figure 11 : Difference between time-gap and safe time-gap	26
Figure 12 : Modified IDM Model in Stationary State	27
Figure 13 : Bottleneck recognition.....	29
Figure 14 : No-Control Case: Spatio-temporal diagram of speed for 0% penetration rate.....	31
Figure 15 : No-Control Case: Spatio-temporal diagrams of speed considering various Penetration Rates (PR).....	32
Figure 16 : Traffic Control Case 1: Spatio-temporal diagrams of speed considering various Penetration Rates (PR).....	36
Figure 17 : Traffic Control Case 1: Spatio-temporal diagrams of time-gap considering various Penetration Rates (PR).....	37

Figure 18 : Time-trajectory of the outflow from the merge (congested) area.....	38
Figure 19 : Capacity flows for No-traffic Control and Control Case 1, for various Penetration Rates	38
Figure 20 : Traffic Control Case 2: Spatio-Temporal Diagrams of speed considering various Penetration Rates (PR).....	42
Figure 21 : Traffic Control Case 2: Spatio-Temporal Diagrams of time-gap considering various Penetration Rates (PR).....	43
Figure 22 : Capacity flows for No-traffic Control and Control Case 2, for various Penetration Rates	44
Figure 23 : Traffic Control Case 3: Spatio-temporal diagrams of speed considering various penetration rates (PR)	46
Figure 24 : Capacity flows for No-traffic Control and Control Case 3, for various Penetration Rates	47
Figure 25 : Traffic Control Case 4: Spatio-temporal diagrams of speed considering various Penetration Rates (PR).....	50
Figure 26 : Traffic Control Case 4: Spatio-temporal diagrams of time-gap considering various Penetration Rates (PR).....	51
Figure 27 : Capacity flows for No-traffic Control and Control Case 4, for various Penetration Rates	52
Figure 28 : Discharge flows for the No-Traffic Control and Complete Traffic Control Case, for various Penetration Rates (PR).....	54
Figure 29 : Traffic Control Case 5 (Full Control Case): Spatio-temporal diagrams of speed considering various Penetration Rates (PR)	55
Figure 30 : Traffic Control Case 5 (Full Control Case): Spatio-temporal diagrams of time-gap considering various Penetration Rates (PR)	56
Figure 31 : Discharge flows for the No-Traffic Control and all Traffic Control Cases, for various Penetration Rates (PR).....	60

List of Tables

Table 1: No-Traffic Control Case: Average Vehicle Delay (AVD) and Total Fuel Consumption (TFC) considering various Penetration Rates	30
Table 2: Traffic Control Case 1: Average Vehicle Delay (AVD) and Total Fuel Consumption (TFC) considering various Penetration Rates (PR).....	33
Table 3 : Traffic Control Case 1: Comfort Criteria considering various Penetration Rates (PR).....	34
Table 4: Control Case 2: Average Vehicle Delay (AVD) and Total Fuel Consumption (TFC) considering various Penetration Rates (PR)	40
Table 5 : Traffic Control Case 2: Comfort Criteria considering various Penetration Rates (PR).....	41
Table 6: Control Case 3: Average Vehicle Delay (AVD) and Total Fuel Consumption (TFC) considering various Penetration Rates (PR)	45
Table 7: Control Case 4: Average Vehicle Delay (AVD) and Total Fuel Consumption (TFC) considering various Penetration Rates (PR)	48
Table 8 : Traffic Control Case 4: Comfort Criteria considering various Penetration Rates (PR).....	49
Table 9: Control Case 5: Average Vehicle Delay (AVD) and Total Fuel Consumption (TFC) considering various Penetration Rates (PR)	53
Table 10 : Traffic Control Case 5: Comfort Criteria considering various Penetration Rates (PR).....	54
Table 11: Traffic Control Cases.....	58
Table 12 : No-Traffic Control and Control Cases: Average Vehicle Delay (AVD) and Total Fuel Consumption (TFC) considering various Penetration Rates (PR)	59
Table 13 : Traffic Control Cases: Comfort Criteria considering various Penetration Rates (PR)	61

Abstract

Traffic congestion is a severe problem which has emerged due to the continuously increasing number of vehicles on motorways in many countries. In most cases, the construction of new transport infrastructure is not an option. In order to improve the traffic conditions on motorways, research has been performed on intelligent transportation systems. An aspect of these systems are Adaptive Cruise Control (ACC) Systems, which are, at present, mainly designed to increase the driving safety and comfort.

This thesis presents an ACC-based traffic control strategy, which aims to adapt in real time the driving behavior of ACC-equipped vehicles to the prevailing traffic conditions so as to increase traffic flow efficiency if and where needed. The ACC system acts automatically and adjusts the vehicle's acceleration or deceleration so as to maintain either the desired maximum speed or the desired time-gap to the leading vehicle. The proposed control concept receives real-time traffic measurements from motorway sections and suggests to the drivers, or imposes directly, appropriate values for the time gap and modified acceleration dynamics, within acceptable safety limits. It should be stressed that the strategy intervenes only when needed, i.e. only when the motorway traffic flow efficiency needs to be improved so as to avoid or mitigate congestion. While demonstrating the potential benefits that may arise by applying the proposed control concept, different ACC penetration rates are used. Microscopic simulation is applied to a real motorway stretch (Motorway A20 in The Netherlands) where recurrent traffic congestion is created under the current manual-driving conditions due to an on-ramp bottleneck.

The simulation results demonstrate that for various, even low, penetration rates of ACC-vehicles, the proposed control concept improves the traffic conditions in general. Specifically, the average vehicle delay and the total fuel consumption have lower values compared to the case of only manually-driven or regular ACC-vehicles. This improvement is achieved by retarding the onset and reducing the space-time extent of the congestion in comparison to the no control case.

1. Introduction

1.1 Motivation

Human civilization has always been reliant, even from ancient times, on transport operations to carry out important tasks. Nevertheless, in the last few years and especially after the second half of the 20th century, the appearance of traffic congestion, due to the increase in the number of vehicles and traffic demand, has led to impact people's quality of life. For the reasons stated above the resolve of this continuously growing problem was deemed necessary.

In order to improve the traffic conditions on motorways, research has been performed on intelligent transportation systems (ITS). These systems include Adaptive Cruise Control Technology (ACC) which aims to create an "intelligent" way of increasing the network capacity. In the near future the number of vehicles equipped with this technology will sharply increase. When following slower vehicles the drivers are able to adjust the desired maximum speed and time-gap to the leading vehicle by using the ACC systems. These systems extend the functionalities of earlier cruise control systems. With the advance of technology even more capabilities will be given to the users (drivers or traffic operators).

The ACC system acts automatically and adjusts the vehicle's acceleration or deceleration so as to maintain either the desired maximum speed or the desired time-gap to the leading vehicle, based on the driver's settings and current measurements. For the time being the ACC systems are mainly designed to increase the driving safety and comfort, therefore some conservative values for the ACC system settings may be used, i.e. comparatively large time-gaps and low accelerations. For example, the typical default time-gap value in vehicles equipped with the ACC technology is usually higher than 2 seconds. Such values can be considered conservative and may lead to the eventual degradation of the static dynamic road capacity compared with conventional manual-driving vehicle traffic. The higher the percentage of the ACC vehicles (penetration rate), the more pronounced will be the influence of their driving modus on the overall traffic flow.

In opposition to the vast literature on ACC and CACC (Cooperative Advanced Cruise Control) systems, which focuses on the design, functionality or architecture of these systems, there is a comparatively small number of works which investigate the impact of ACC and CACC systems on traffic flow. The main purpose of this research is to capture the impact of ACC on traffic flow under different settings, mainly different time-gaps, and penetration rates, using either microscopic simulation [1]–[10] or macroscopic approaches [11]–[15]. We can conclude from these works the following: 1. The ACC systems have the potential to improve or deteriorate, depending on their settings, the traffic conditions compared to the case of conventional manually driven vehicles and 2. the level of influence is closely related to the ACC penetration rate. However, the above studies do not systemically examine how the ACC settings should be, actually specified.

This direction is examined in few studies [16], [17], which propose the offline optimization of the (constant) ACC system parameters so as to maximize the traffic flow efficiency. They show that with the appropriate use of the ACC technology and the optimal settings the network's traffic performance may indeed be improved. Finally, there are a few more studies [18]–[21] which incorporate the above but also attempt to change the ACC settings in real-time, based on the prevailing traffic conditions, in order to improve the traffic flow efficiency. These studies have two main ways of addressing the problem. The first one is to consider advisory systems, located in a traffic management centre, which provide action advice, i.e. change of ACC system settings to vehicles featuring appropriate automation and connectivity capabilities (as in [18], [19]). The second way is to consider the autonomous operation of individual ACC equipped vehicles, which based on a vehicle-based detection algorithm, identify the traffic conditions and adapt appropriately their individual settings (as in [20], [21]). The corresponding approaches require except for real-time traffic data, also topology information for their functional operation, i.e. on ramps and off ramps and lane drop locations.

1.2 Thesis Objectives

The objective of this thesis is the creation of a simple and effective ACC-based control strategy. This strategy aims to adjust in real time the driving behavior of ACC-equipped vehicles to the prevailing conditions so as to increase traffic flow efficiency if and where needed. The proposed control concept consists of two parts. In the first part we leave the ACC settings untouched at their driver selected values if the traffic flow is clearly under its critical value. By doing so we limit our interventions to the network and we only interfere to traffic situations that call for efficiency increase. This concept leads to an outflow increase. The second part is to change the ACC settings gradually according to the traffic situation in order to improve the flow efficiency when facing critical traffic states. By doing so, a significant road capacity increase is achieved. The complete control strategy depends only on real-time information about the current traffic conditions, in contrast to [20], [21], hence, no network topology information is required and it is activated only when, where and to the extent needed. This approach to the control concept is validated using a real network simulation model and it is tested using the microscopic traffic simulator AIMSUN through scenario simulations.

1.3 Thesis Outline

This thesis is composed of 5 sections. Section 1 is the introduction in which we describe the general problem as well as the motivation and the goals for this thesis. Also this section includes the review of relevant literature. In Section 2, the proposed ACC-based control concept is presented. At the beginning we present the individual concepts concerning the time-gap and the acceleration, as well as the equations needed to implement them. Section 3 is a brief description of the AIMSUN microscopic traffic simulator. Furthermore in this section we describe the network and the IDM model with its parameters, which is used throughout this study in order to implement our strategy. In Section 4 the simulation results are presented. Finally in Section 5 we summarize the conclusions of this study.

2. Methodology

2.1 Traffic Control Concept

Research has showed that the ACC systems, if used correctly, have the ability to improve the traffic conditions on a motorway. Such improvements may be the smoothing of traffic flow, decreasing fuel consumption and improving the efficiency overall. Furthermore by using the ACC vehicles and their technology, which can in real time implement the suggested strategy, the driving safety and comfort is increased. Nevertheless, if the drivers or the strategy set conservative values for the parameters, such as the desired time-gap, then the ACC technology may worsen the traffic conditions and lead to the deterioration of the network. For example, the drivers of the ACC vehicles can select their desired time-gap to the front vehicle which may vary from 0.8-2.2 s [22] but the default time-gap setting is higher than 2s. Furthermore, some drivers may be selecting ACC time-gaps that are higher than those employed in manual driving. Applying these conservative time-gap settings suggest that the vehicles maintain a significant distance to their front vehicle and this could lead to the decrease of the motorway capacity per lane because the network can now accommodate less vehicles. In order to mitigate this impact, a real-time ACC based control concept is established. Through that the settings of the ACC-vehicles can be updated dynamically in real time.

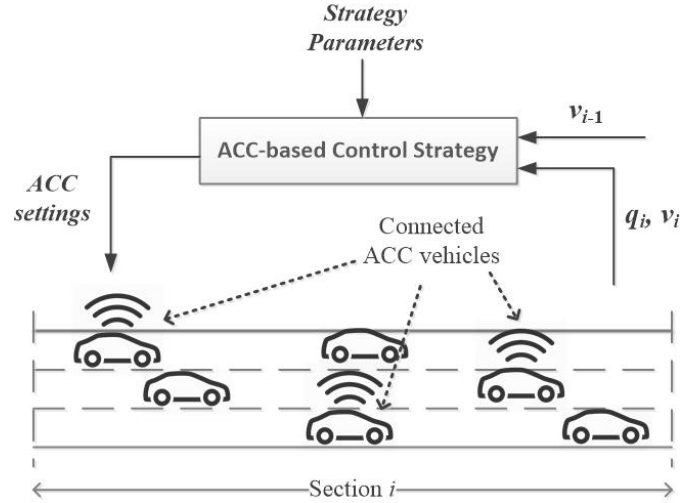


Figure 1 : Illustration of the control system operation

For the purposes of the control strategy, consider a motorway divided in sections i . At every section there is a percentage of ACC cars meddled with the manual cars. The ACC-vehicle drivers have the choice to introduce their desired system settings, for example the desired speed v_d , the minimum time gap T_d , however the latter is not a fixed value and may be subjected to changes if the control strategy recommends or orders a lower time-gap. The proposed control strategy is applied at every motorway section independently, as illustrated in **Figure 1**. In particular, at every period or control interval t_c , the strategy receives real-time measurements, or estimations, of the entering flow q_i and speed v_i of every section i . These measurements are acquired either through ordinary loop detectors, or may be estimated through the V2I communication (Vehicle to infrastructure communication) [23]. (The vehicle to infrastructure interaction is a communication model that allows vehicles to share information with the components that support the highway system.). **Figure 1** illustrates the proposed strategy goals.

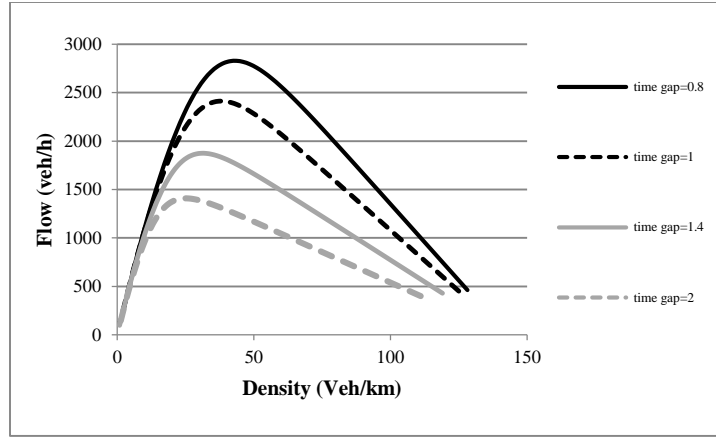


Figure 2 : Single-lane fundamental diagram for various time-gaps

Figure 2 displays a single-lane fundamental diagram for various time-gaps, which results as a stationary version of the IDM (Intelligent Driver Model) to be presented in detail later in chapter 4. It is shown that lower time-gaps lead to higher capacities. For example, there is a lane capacity of 1410 veh/h for a time-gap of 2 s, while for a time-gap of 0.8 s the lane capacity is 2830 veh/h. From the first example we get a lane capacity which is drastically lower from the typical of manually driven vehicle traffic. Whereas, from the second example the lane capacity is drastically higher. These values are only rough estimates, but it is clear that any reduction of the time-gap applied by ACC vehicles increases the motorway capacity. Furthermore, the adoption of the minimum allowed time-gap of 0.8 s would lead to a maximum achievable capacity value for all the penetration rates of ACC vehicles (percentage of ACC vehicles meddled with manual driven vehicles). The proposed control strategy determines in real time the time-gaps of the ACC vehicles that lead to the increase of the static and dynamic road capacity, where and when it is needed.

The strategy is divided into two main concepts. For each concept different parameters are tested.

2.1.1 Capacity increase

The main concept of this strategy is to delay or even prevent the congestion from formatting by attempting to gradually decrease the suggested time-gap when the traffic flow is within certain bounds. Specifically, the strategy calculates the suggested time-gap as function of the current section flow, $T_i[q_i(k)]$ and intervenes only when needed, i.e. when being out of congestion

$v_i > v_{cong}$. In **Figure 3** it is shown the strategy reduces the suggested time-gap while the flow q_i increases, using a linear function. In this function there is an upper and a lower flow bound. When the flow is below the lower limit Q_1 (i.e. $q_i \leq Q_1$) the strategy suggests the maximum time-gap T_{max} , since traffic is not critical. For high flow values (i.e. $q_i \geq Q_2$) the strategy suggests the minimum time-gap T_{min} . It should be stressed that the minimum time-gap value is imposed before the flow reaches the normal capacity, for the manual vehicles. When the congestion starts then the strategy does not intervene and the vehicles behave similar to their corresponding no control case. By doing so, the strategy aims to avoid or mitigate congestion, by maximizing timely the section's capacity.

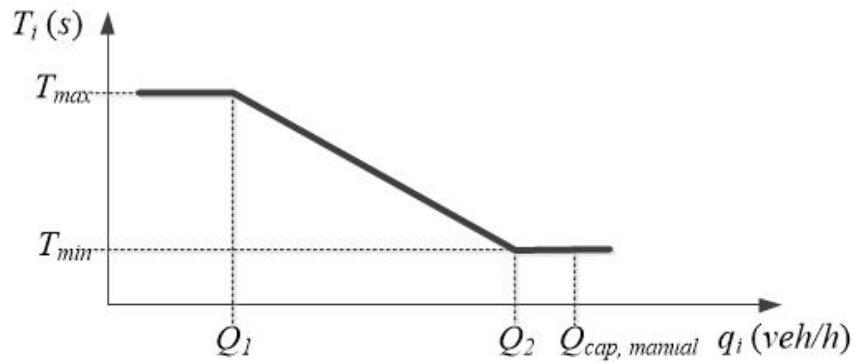


Figure 3 : Calculation of the suggested time-gap value using a linear function

The proposed function of time-gap versus flow can be replaced by a decreasing stepwise function. As shown in **Figure 4**

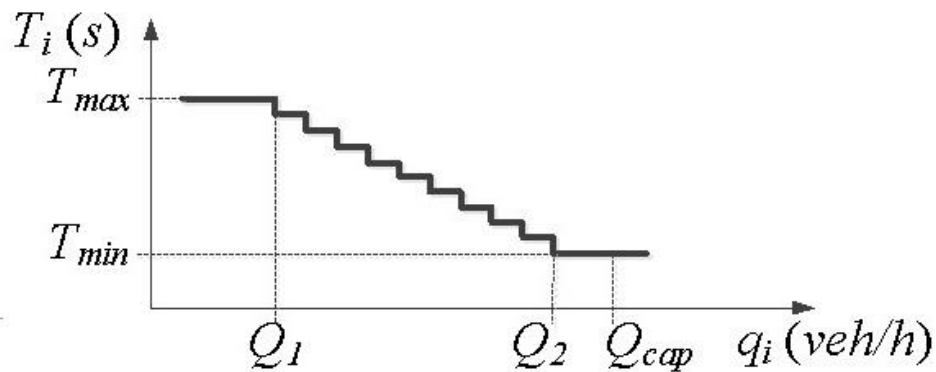


Figure 4 : Calculation of the suggested time-gap value using a stepwise function

By using the stepwise function we get more frequent but less abrupt gap changes when working with higher values. However if the section becomes congested despite the capacity increase, the strategy suggests the maximum time-gap T_{max} , for safety reasons. The above mentioned congestion could be due to even higher arriving demand or due to a shockwave arriving from downstream. We summarize the above control decisions by using the following equation which determines the suggested time-gap

$$T_{stg,i}(k) = \begin{cases} T_i[q_i(k)] & \text{if } v_i(k) > v_{cong} \\ T_{max} & \text{else} \end{cases} \quad (1)$$

Where $k=1,2,\dots$, is the discrete time index and v_{cong} indicates the congestion limit. The decisions on whether impose the maximum or minimum time-gap are calculated externally, at an infrastructure-based traffic management center (or road-side unit) and are disseminated to the ACC vehicles, via V2I communication.

2.1.2 Increase discharge flow

The main goal of this strategy is the maximization of the discharge flow during congestion at the location of active bottlenecks (dynamic capacity). It is empirically known that the discharge flow at the head of a congested area is lower than capacity, and the second goal is to mitigate this capacity drop. The strategy first identifies the location of active bottlenecks. More specifically, if two consecutive sections $i - 1$ and i , have a speed difference higher than a threshold Δv , and the mean speed $v_i(k)$ of downstream section i is higher than the congestion speed v_{cong} , while the mean speed of the upstream section, $v_{i-1}(k)$, is lower than v_{cong} , this indicates that these two sections are located just upstream and just downstream of the head of a congested area, i.e. that an active bottleneck has been identified. **Figure 5** illustrates the sections in which the congestion head is detected.

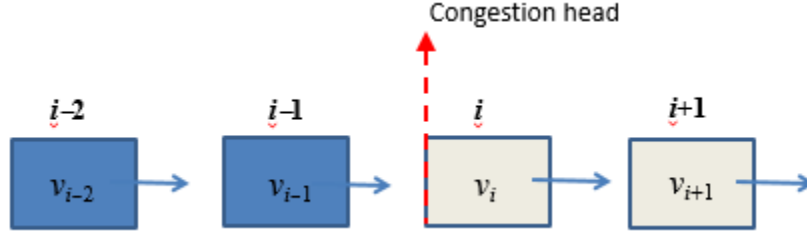


Figure 5 : Detection of the congestion head

The discharge flow at the congestion head can be increased with two independent strategies which can be implemented separately or at the same time. The first strategy suggests the minimum time-gap T_{min} and the second increases the acceleration at all ACC vehicles, both for the two mentioned sections. These extended control decisions are implemented via the following relations:

$$IF v_i(k) > v_{cong} \text{ AND } v_{i-1}(k) < v_{cong} \text{ AND } [v_i(k) - v_{i-1}(k)] > \Delta v$$

$$T_{stg,i}(k) = T_{min} \text{ or/and increase the section's } i \text{ acceleration} \quad (2)$$

$$T_{stg,i-1}(k) = T_{min} \text{ or/and increase the section's } i - 1 \text{ acceleration}$$

To avoid possible oscillations or false alarms due to moving shock waves, the speed measurements or estimates are sufficiently smoothed before being used.

The two equations give us the suggested time-gap value at each control period, however the value applied to the ACC cars is the minimum value between the suggested and the one set by the driver. As a result the suggested time-gap is not always applied.

$$T_{applied,j} = \min\{T_{d,j}, T_{stg,i}\} \quad (3)$$

where $j=1,2,\dots$ is the ACC vehicle index. The advancing ACC vehicles update their time-gap settings, using the relations explained above, in a frequency that may be higher than every control

interval t_c . This happens because of the crossing of section boundaries, unless the broadcasting of centrally calculated time-gaps is only executed at every t_c strictly.

The proposed control concept is simple and easy to implement. It considers real time communication between the ACC-vehicles and the traffic management centre which suggests to the drivers (or imposes directly) appropriate values for the ACC parameters. It requires only real-time flow and speed measurements (or estimates) from the motorway sections, and is activated only when, where and to the extent needed [24].

The strategy includes four parameters that should be appropriately specified, i.e. $Q_1, Q_2, v_{cong}, \Delta v$; while T_{min}, T_{max} are naturally set equal to the bounds of commercial ACC systems. The choice of the Q_1 and Q_2 parameters influences the amount and level of required time-gap changes. The values of v_{cong} and Δv might need some easy fine-tuning for different traffic infrastructures. The sensitivity of results with respect to these parameters was found to be minor in the following investigations.

3. Application

3.1 Aimsun

The microscopic traffic simulator AIMSUN (Advanced Interactive Microscopic Simulator for Urban and Non-Urban Networks) [25] was used for the purposes of this study. AIMSUN's microscopic simulator can continuously model the behavior of each vehicle in the network during the simulation time period [26]. AIMSUN is a combination of discrete and continuous simulator, this means that there are elements such as vehicles and detectors that their state constantly changes over the simulation period. The simulation period is divided into small fixed time intervals, those intervals are called simulation steps. Furthermore there are elements whose state changes discretely over the simulation time such as traffic signals and entrance points. Overall AIMSUN can depict in detail a traffic network as well as the elements that exist in real life networks. Such elements are detectors, traffic lights, traffic signs etc.

AIMSUN API (Application Programming Interface) is used for the communication between the microsimulator and the user during the simulation. Through this interface the user can get useful information about the vehicles or the demand and then set the appropriate strategy. Before setting the strategy, the user can appoint an external application to access the data of AIMSUN. This application is considered to be a signal control strategy which requires dynamic changes of its situation.

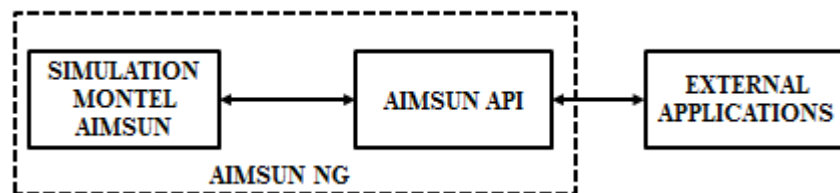


Figure 6 : Conceptual Diagram of AIMSUN API

The AIMSUN API has two directions of communication. The first one is between the AIMSUN's simulated model and the API. The second one is between the AIMSUN API and the

external applications (i.e. a signal control strategy) (**Figure 6**). In both cases the communication is bidirectional and the two sides interact with each other.

The microSDK simulator (Software Development Kit) is used for the modification of the behavioral models of the desired vehicles. By using the microSDK simulator we can intervene in every vehicle and set the lane changes, the acceleration, and the deceleration of the ACC vehicles as well as the time gap. With the completion of the simulation, the data generated as program outputs are the total fuel consumption and the delay. The total fuel consumption is the sum of the fuel consumption from each car in the network and the delay corresponds to the average time that the vehicles needed to cross the network.

3.2 Network description

The simulated network is a part of the A20 motorway in The Netherlands, which connects Rotterdam and Gouda. The motorway stretch considered is about 9.3 km long and it includes two on-ramps and two off-ramps. It features 3 lanes until its 3.6 km, where the left-most lane drops (see **Figure 7**).

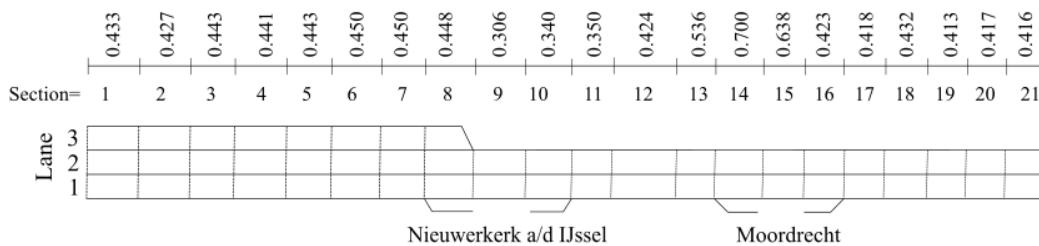


Figure 7 : Sketch of the Motorway A20 in The Netherlands

On the examined stretch the analysis shows that recurrent congestion is created during the morning peak hours [27] . The congestion is created because on the first on-ramp appears a high demand, which combined with the mainstream demand, exceeds the motorway capacity.

In order to test the proposed control strategy concept we use the real motorway stretch. Through the study of the network, real traffic data have been acquired, these data are used to calibrate and validate the microscopic simulator AIMSUN. By doing the above, we are able to reproduce the typical traffic evolution under manual driving conditions. [27], [28]

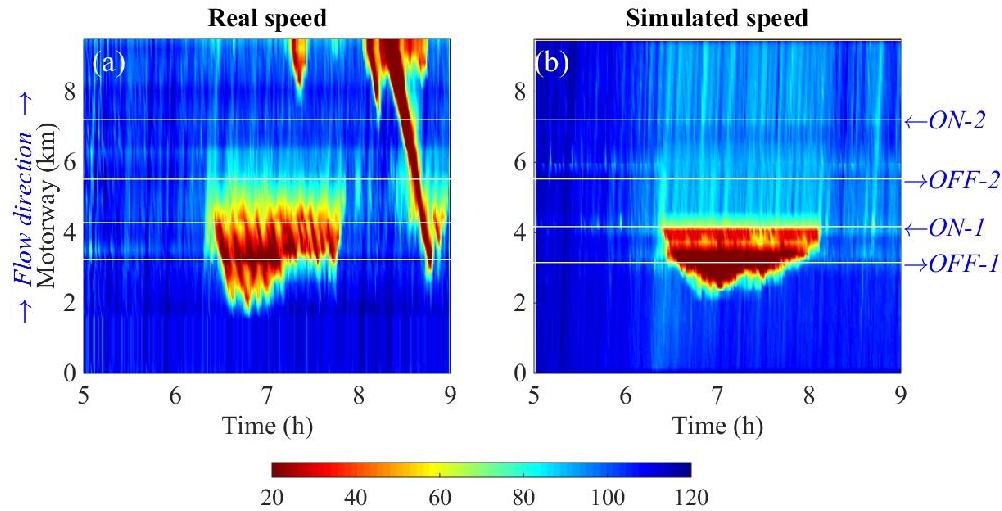


Figure 8 : (a) Spatio-temporal diagrams of real speed (b) Spatio-temporal diagrams of simulated speed

The above figures are spatio-temporal diagrams of speed. These diagrams are three dimensional, the x axis represents time, measured in hours, the y axis represents the flow direction, measured in kilometers and the colors show the speed of the vehicles. According to the index the color red reflects low speeds (where we have congestion) and as the scale goes further we have higher speeds, with the highest being represented in blue color.

Figure 8a illustrates the spatio-temporal diagram of the examined network's real speed whereas **Figure 8b** illustrates the corresponding diagram of the simulated speed which is obtained through the calibrated simulator. By comparing these figures we detect that the microsimulator succeeds in formatting the congestion at the first on-ramp for the correct time, period and extend. It should be pointed out that this study focuses only on the bottleneck created due to the on-ramp merge and not the second wave of congestion which enters the examined motorway from the downstream boundary (see **Figure 8a**). Therefore the second wave is excluded from the

simulated model and the microsimulator AIMSUN assumes free-flow traffic conditions downstream of the motorway stretch at all times.

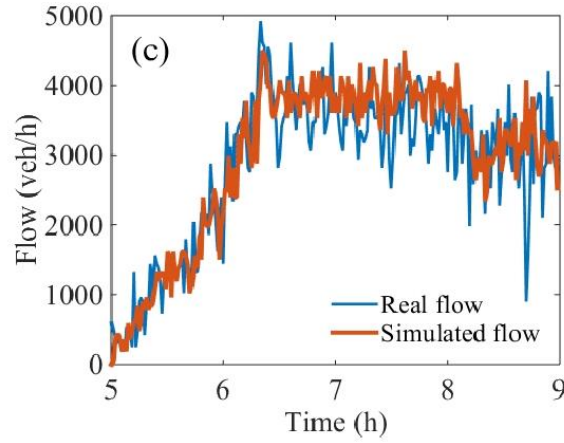


Figure 9 : Real and simulated outflow from the merge area

Furthermore, **Figure 9** illustrates the time trajectory of the outflow from the congested area for the real as well as the simulated flow. It is shown that the outflow, for both cases, during the congestion period, is reduced below the motorway capacity. Thus we have a capacity drop.

3.3 IDM Model

For the purposes of this study the ACC vehicles as well as the manual ones are moving using the IDM Model (Intelligent Driver Model)[29]. This model is one the simplest, accident free and most easy to understand car-following models. It has been used from many researchers especially for modelling manual vehicles. The IDM calculates the vehicle acceleration \dot{v} based on the following equation:

$$\dot{v}(s, v, \Delta v) = \alpha \left[1 - \left(\frac{v}{v_0} \right)^4 - \left(\frac{s^*(v, \Delta v)}{s} \right)^2 \right] \quad (4)$$

Where α is the maximum acceleration, v_0 is the desired speed, s is the current distance to the proceeding vehicle and $s^*(v, \Delta v)$ is the desired distance which is calculated by the following function:

$$s^*(v, \Delta v) = s_0 + vT_s + \frac{v\Delta v}{2\sqrt{ab}} \quad (5)$$

Where s_0 is the minimum distance, T_s is the safe time gap and b is the comfortable deceleration. In stationary state the acceleration and Δv are zero, thus from equation (4) we have:

$$1 - \left(\frac{v}{v_0}\right)^4 - \left(\frac{s^*}{s}\right)^2 = 0 \quad (6)$$

Also from equation (5) we get

$$s^* = s_0 + vT_s \quad (7)$$

By replacing this equation in equation (6), we get the stationary gap (given in meters)

$$s = \frac{s_0 + vT_s}{A}, \text{ with } A = \sqrt{1 - \left(\frac{v}{v_0}\right)^4} \quad (8)$$

Therefore the stationary time gap (given in seconds) is

$$T_{real} = \frac{s}{v} = \frac{T_s + \frac{s_0}{v}}{A} \text{ with } 0 \leq A \leq 1 \quad (9)$$

Furthermore, in stationary state it is understood from equation (5) that the theoretical time gap (the time-gap ordered by the user) that is produced by the choice of T_s is equal to

$$T_{th} = T_s + \frac{s_0}{v} \quad (10)$$

Finally, by replacing equation (10) to equation (9) we get

$$T_{real} = \frac{s}{v} = \frac{T_{th}}{A} \text{ with } 0 \leq A \leq 1 \quad (11)$$

It is worth noting that all IDM parameters i.e. v_0, T_s, s_0, a and b take positive values. Within AIMSUN simulator, these parameters are defined by a mean, maximum and minimum value, while the characteristics for each individual vehicle are sampled from a truncated normal distribution.

From equations (10) and (11) it is obvious that the calculated time-gap T_{real} , which derives from the IDM, will be different from the theoretical value T_{th} and also different from the safe time-gap T_s . These differences are illustrated in **Figure 9**. Generally in most models the time gap can be fixed to the desired value, for example $T=0.8$ s. Nevertheless because of the term $A = \sqrt{1 - \left(\frac{v}{v_0}\right)^4}$ which was used in the model analysis, the IDM model gives a different time gap than the one ordered by the user, especially when $\left(\frac{v}{v_0}\right) \rightarrow 1$, even for the stationary case.

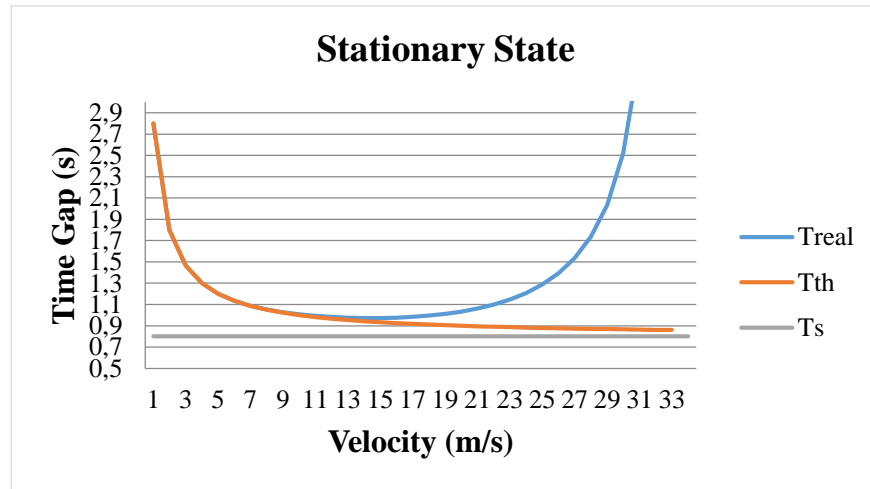


Figure 10 : IDM Model in Stationary State

Another problem that can be found in the literature is the difference between T and T_s . Several researchers seem to use the safe time-gap T_s instead of T . In the bibliography, there seems to be a misunderstanding and this difference is not clearly determined by the researchers. It is observed that while $T_s = 0.8$ s is defined as safe time gap, $T = 0.8$ s is considered to be the same. For example at [30], the researchers claim that IDM produces a high time-gap error:

“This large gap variation raises questions about the driver acceptance of the IDM as an automatic car-following control strategy. Although IDM+ or IDM models could improve this behavior (because they include specific modifications to deal with this time-gap error), the big delay introduced by the onboard sensors and the undershoot that is detected in the last braking maneuver would be amplified when ACC-equipped vehicles (using the IDM+ or IDM systems)

drive consecutively. This result suggests that when ACC market penetration increases it will not improve traffic flow, but will rather cause it to become less stable.”

Contradicting the above, we already shown in **Figure 10**, that this high time-gap error derives from the wrong usage of the various types of time-gaps. In order to clarify this matter, **Figure 11** illustrates the difference between time-gap and safe time-gap.

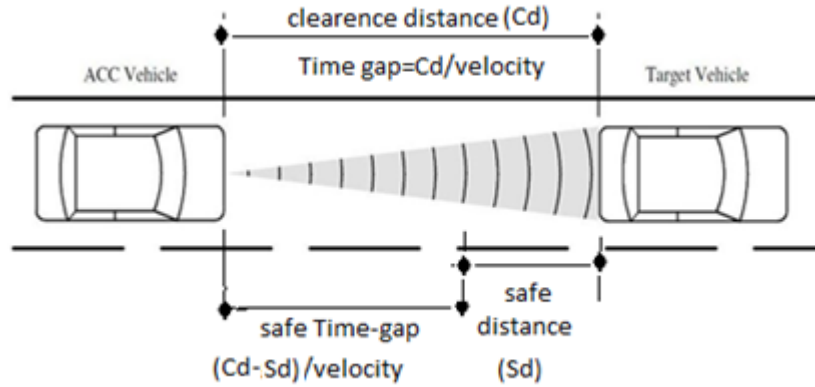


Figure 11 : Difference between time-gap and safe time-gap

Figure 10 illustrates the difference between the time-gap the IDM produces T_s and the theoretical T_{th} in stationary case. It is observed that for velocities lower than the critical that $T_{th} \cong T_{real}$ and for velocities higher than the critical the time-gap values are completely different. Whichever the case, the theoretical and the real time-gap are always different from the safe time-gap value T_s , which is given by the user.

According to the above, it is imperative we make a new formulation for the IDM model so that there is a connection between the various time gaps. The new model formulation, which replaces equation 5, is

$$s^* = \min \left(s_0, vT + \frac{v\Delta v}{2\sqrt{ab}} \right) \quad (12)$$

From equations 4 and 12 we get the same IDM benefits (accident free model, simplicity, physical meaning of all the parameters) plus now we can be sure about the time-gap value ordered by the user hence now it is independent from the vehicle speed.

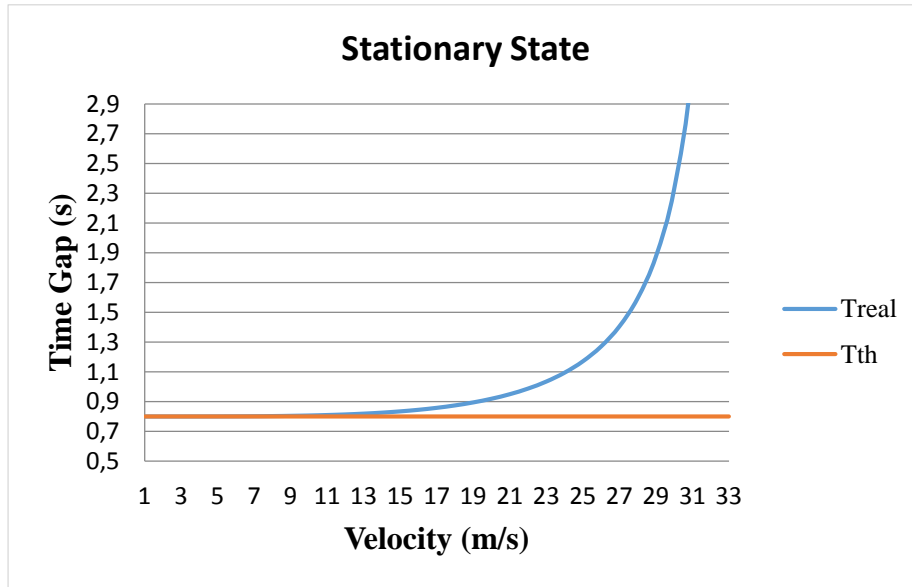


Figure 12 : Modified IDM Model in Stationary State

Figure 12 illustrates the theoretical (ordered) value versus the real value of time-gap for the modified IDM. In this figure we observe that the real time gap is almost identical with the theoretical for velocities which lower of the critical one ($T_{real} \approx T_{th}$). For velocities over the critical velocity we have $T_{real} \neq T_{th} = T_{ord}$. Note that Figures 10 and 12 come of an example that uses $s_0 = 2\text{ m}$, $T_{ord} = 0.8\text{ s}$, $v_0 = 33.33\text{ m/s}$ with $T_{ord} = T_s$ for **Figure 9** and $T_{ord} = T_{th}$ for **Figure 11**.

3.4 Simulation Set-up

The manual vehicles are moving using the IDM car-following model (equations 4 and 5) whereas the ACC vehicles are moving using the modified IDM car-following model. This model

was chosen for both types of vehicles in order to ensure that the discovered results are because of the time-gap policy and not because of a different ACC dynamic vehicle model taking effect. In the investigations we are mainly interested in the impact the time-gap and the maximum acceleration have to the congestion. In order to achieve that we employ the IDM equation also for the ACC vehicles.

Now that the car-following equations of the ACC vehicles are known, we can express with more details the control equation 2 and especially the phrase “*increase the section’s i acceleration*”. In case of active bottleneck the max acceleration of the vehicles is doubled just before and just after the head of congestion and the below formulation is used:

$$\dot{v}(s, v, \Delta v) = \min \left(acc_{\max}, 2a \left[1 - \left(\frac{v}{v_0} \right)^4 - \left(\frac{s^*(v, \Delta v)}{s} \right)^2 \right] \right) \quad (13)$$

where acc_{\max} is an upper bound for the ACC vehicles acceleration and for our simulations it is set to 2.5 m/s^2 . Note that a (or $2 \cdot a$ for the case of active bottleneck) is the higher possible value that IDM can give to the vehicle acceleration and in this work it is assumed that every ACC-driver can choose her own maximum acceleration. A truncated normal distribution has been used with $\alpha \in [1.13, 2.13]$ with mean value 1.63 m/s^2 .

For different ACC models, the parameters of the model that produce the acceleration of the ACC vehicles, has to be treated with the appropriate way to increase the acceleration. By using IDM this procedure is simpler and with physical meaning because the change of the produced acceleration is direct.

The difference between the manual and the ACC vehicles are the distribution bounds for the time-gap value. For the manual vehicles the distribution bound for the safe time-gap is $T_s \in [0.48, 1.52]$ with mean value $T_s = 1$, so the real time-gap bound is $T_{real} \in [0.63, 1.67]$ with mean value $T_{real} \cong 1.15$. For the ACC vehicles the distribution bound for the time-gap is $T \in [0.8, 2.2]$ with mean value $T = 1.4$ and standard deviation 0.3 s . The range of time-gap values for the manual vehicles coincides with the typical values derived from the calibrated network, while the mentioned range of values for ACC-vehicles delivers a mean value that is comparable

with the one found empirically to be employed by the users [31]. The utilized AIMSUN simulation step was set to 0.4 s, while the control period was set to 30 s. For the cases where the congestion speed is needed $v_{cong} = 60 \text{ km/h}$. By applying our bottleneck recognition strategy to the network we get the following graphs.

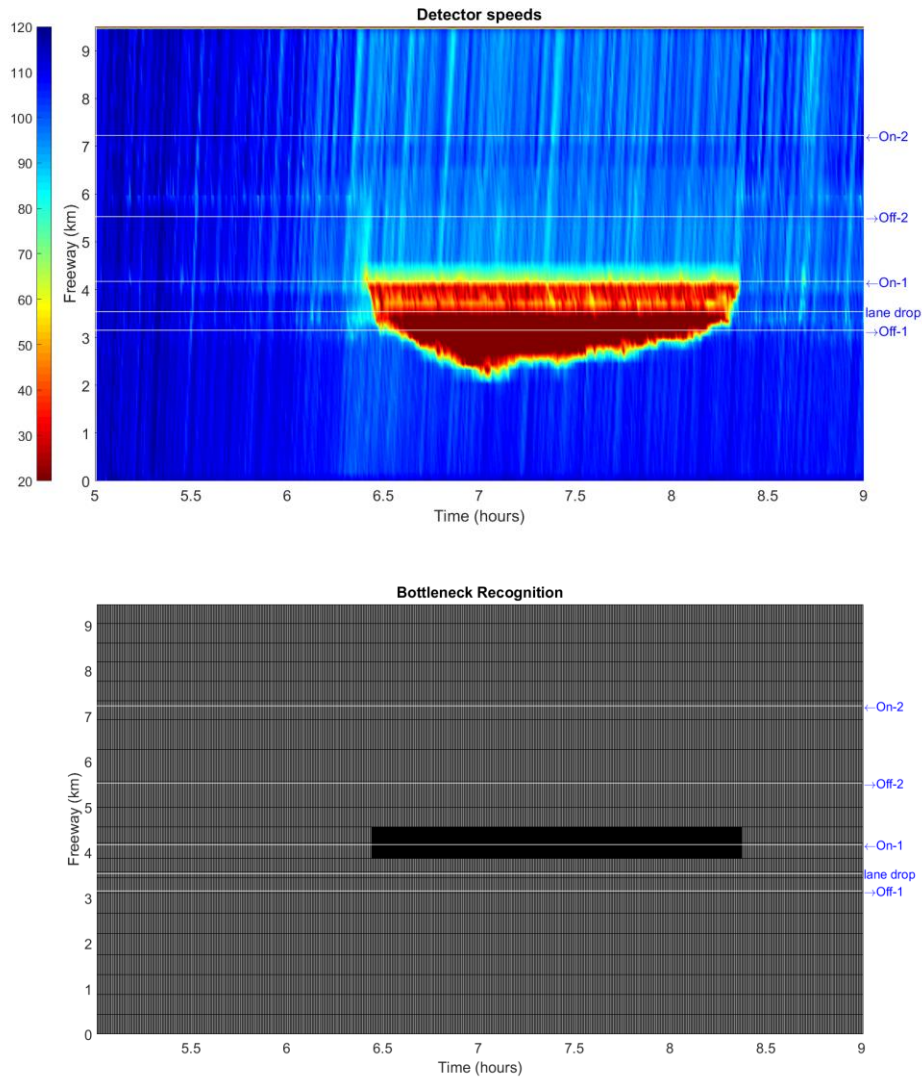


Figure 13 : Bottleneck recognition

From **Figure 13** it can be observed that the control concept succeeds in recognizing the bottleneck. The black line in the lower graph shows that the bottleneck is created right before the first on-ramp. It should be noted that the black line consists of the following upstream and downstream bottleneck sections. Furthermore, by comparing the two graphs we can conclude that the time in which the bottleneck recognition is achieved is precise.

4. Simulation Investigations

In this chapter the simulation results of all the Traffic Control Cases are presented. The first section concerns the No-Traffic Control Case, followed by the results of applying the first part of the proposed control strategy (Equation 1) and its complete version (Equations 1 and 2), considering various penetration rates (PR). For each of the examined scenarios the average values of the performance criteria are compared. These values are derived from ten replications carried out by the AIMSUN microscopic traffic simulator.

Table 1: No-Traffic Control Case: Average Vehicle Delay (AVD) and Total Fuel Consumption (TFC) considering various Penetration Rates

PR	AVD (s/veh/km)	Difference (%)	TFC (l)	Difference (%)
0%	19.5	-	6786	-
5%	21.1	8.4	6785	-0.02
10%	21.3	9.0	6786	0
20%	24.3	24.5	6787	0.02
30%	27.1	38.9	6813	0.4
60%	44.4	127.1	6886	1.5

4.1 No-Traffic Control Case

In the case without traffic control, 100% manually driven vehicles are considered. The results presented in **Table 1** include the average vehicle delay (AVD) measured in s/veh/km and the total fuel consumption (TFC) measured in l. These estimates are the mean values of 10 replications. Note that, the column Difference (%) states the result change between the case of 0% penetration rate and the corresponding case to be examined.

For 0% penetration rate the average vehicle delay is 19.5 s/veh/km and the total fuel consumption is 6786 l. **Figure 14** illustrates the traffic situation on the motorway for this penetration rate, for a particular replication with AVD value closest to the mean value of the 10 replications.

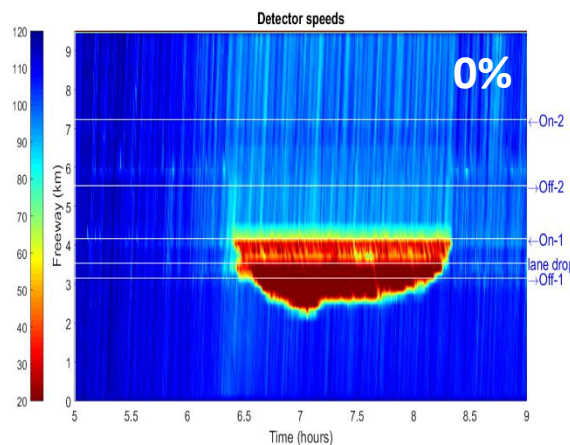


Figure 14 : No-Control Case: Spatio-temporal diagram of speed for 0% penetration rate

According to **Figure 14** the congestion is formed from 6:30 a.m. to 8:30 a.m. at the first on-ramp, which propagates upstream for about 2 km. This figure is identical to **Figure 8(b)** which depicts the calibrated model of the real network problem.

Furthermore, in Chapter 3 it was analyzed extensively that the available range of time-gap values for the ACC vehicles is [0.8, 2.2] s, whose mean value is higher than the calibrated mean value of manually driven vehicles. This suggests that the traffic flow efficiency may be reduced and the conditions worsen. In order to examine this issue, a series of simulation runs were carried out

considering various respective penetration rates of ACC vehicles. **Table 1** presents the Average Vehicle Delay (AVD) and the Total Fuel Consumption (TFC) for each investigated penetration rate. The values represent the mean AVD and TFC values over 10 replications. We can conclude that when the penetration rate of the ACC vehicles gets higher, the bigger the mean AVD and TFC values are. **Figure 15** illustrates the spatio-temporal diagrams of speed considering various penetration rates.

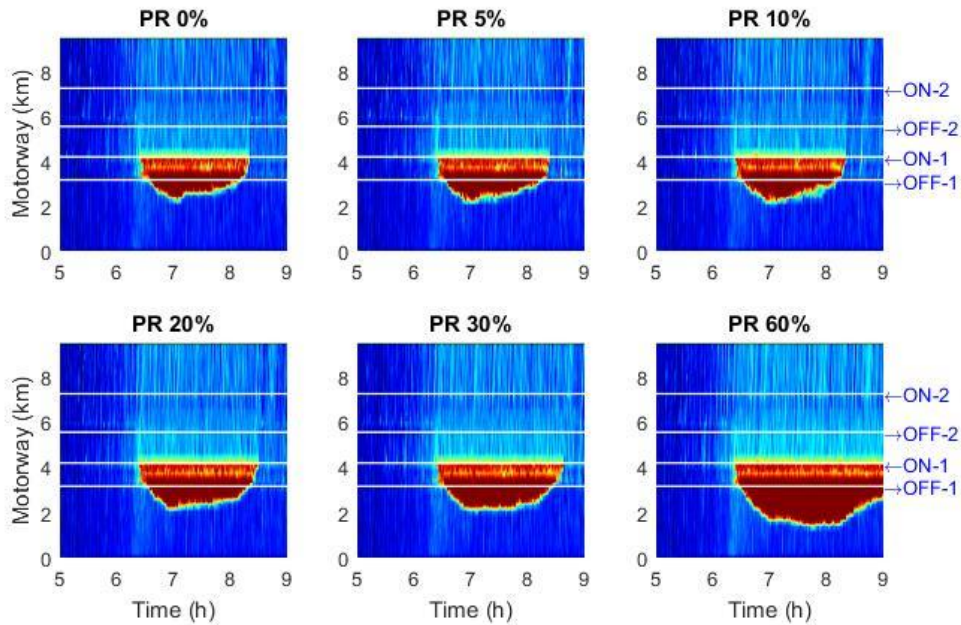


Figure 15 : No-Control Case: Spatio-temporal diagrams of speed considering various Penetration Rates (PR)

The spatio-temporal diagrams depict the increasing AVD values presented in **Table 1**. Moreover, the higher the penetration rate of the ACC vehicles the traffic seems to last longer, until the percentage of ACC vehicles is up to 60% and then we detect the deterioration of the traffic network conditions. In the spatio-temporal diagram considering that particular penetration rate (**Figure 15** bottom right) the traffic congestion does not dissolve. Nevertheless, these findings reject the perception that the introduction of ACC vehicles in the network will automatically improve the driving conditions, as it demonstrates that the “uncontrolled” behavior of ACC vehicles may actually contribute to further degradation of the road infrastructure. By “uncontrolled” behavior we mean the wide range of available time-gap values and the fact that every driver in the network may use a different value appropriate to them.

4.2 Traffic Control Case 1

In traffic control case 1 the concept stated that the appropriate time-gap value should be calculated using equation 1 and that the time-gap value at the bottleneck area should be equal to T_{max} . This strategy aims to increase the static and dynamic road capacity. The application results of the first part of the control strategy are presented in **Table 2**. Note that, the column Difference (%) states the result change between the No-control case and Control Case 1 for each of the Penetration Rates examined.

Table 2: Traffic Control Case 1: Average Vehicle Delay (AVD) and Total Fuel Consumption (TFC) considering various Penetration Rates (PR)

PR	AVD (s/veh/km)			TFC (l)		
	No control	Control case 1	Difference (%)	No control	Control case 1	Difference (%)
0%	19.5	-	-	6786	-	-
5%	21.1	18.7	-11.7	6785	6742	-0.6
10%	21.3	18.5	-12.9	6786	6685	-1.2
20%	24.3	17.7	-27.3	6787	6619	-2.5
30%	27.1	15.9	-41.2	6813	6487	-4.8
60%	44.4	12.0	-72.9	6886	6317	-8.3

Table 3 : Traffic Control Case 1: Comfort Criteria considering various Penetration Rates (PR)

PR	% ACC cars needed time-gap change	How many times the time-gap changed	How much needed to change (absolute value)	% time of having different time-gap than desired
5%	73.8%	6.1	0.30	48.2%
10%	69.2%	6.7	0.28	47.9%
20%	75.4%	7.0	0.27	46.1%
30%	75.3%	7.2	0.26	44.4%
60%	75.4%	7.2	0.26	47.9%

The comfort criteria for various penetration rates are presented in **Table 3**. These criteria show the affect that the applied changes on the network have on the drivers, concerning the time-gap. This table includes only results where ACC vehicles are implemented in the network, due to the fact that time-gap changes can only be applied to such systems. This means that results where the penetration rate is 0% (only manually driven vehicles) are non-existent. It is observed that as the penetration rate gets higher, more vehicles need to change their time-gap. These changes are more frequent and less abrupt and validate the strategy in which the time-gap calculation should be smooth in order to increase the static and dynamic road capacity. However, when the penetration rate is 60% the percentage of time the vehicles had a different time-gap than the desired is high and does not follow the downward trend the results have concerning penetration rates from 5% to 30%. This happens because at 60% penetration rate of ACC vehicles, the congestion is mitigated. We remind that in control case 1 if there is a congested section, the control decisions are not applied for safety reasons.

4.2.1 Controller Settings

The control strategy is activated every $t_c = 30$ s, receiving real-time measurements of flow and speed for every section of the motorway (**Figure 1**), whereby section lengths are around 500 m. The parameters involved in the strategy equations are set as follows: the congestion speed (congestion limit) is $v_{cong} = 60$ km/h, the minimum and the maximum time-gap values are $T_{min} = 0.8$ s, $T_{max} = 2.2$ s respectively. The lower and the upper bounds for the linear function from which the suggested time-gap is calculated are $Q_1 = 1250$ veh/h/lane and $Q_2 = 1700$ veh/h/lane successively. The strategy calculates the suggested time-gap T_{stg} based on Equation 1, using discrete time-gap values from the range $[0.8 - 2.2]$ s with increments of 0.1 s (**Figure 3**). The ACC vehicles receive, every simulation step, the strategy's decisions and update their individual time-gap setting according to Equation 3.

Table 2 presents the Average Vehicle Delay (AVD) in s/veh/km and the Total Fuel Consumption (TFC) in l for each investigated penetration rate. The values represent the mean AVD and TFC values over 10 replications. It is observed that, the higher the penetration rate, the higher the improvement in mean AVD and TFC. Note that, when the penetration rate is 0% the control case does not exist because there are no ACC vehicles in the network, this situation is the same with the corresponding No-Control case. Moreover, the traffic conditions are considerably improved even for 5% penetration rate, where the mean AVD is 11.7% lower compared to the corresponding No-Control case and the mean TFC is 0.6% lower. Furthermore, for a penetration rate equal to 60%, the control strategy manages to achieve 72.9% and 8.3% improvement for the AVD and TFC successively. From the spatio-temporal diagrams we can conclude again that the higher the penetration rate, the bigger the improvement of the traffic condition on the motorway stretch. **Figure 16** displays the above mentioned spatio-temporal diagrams of speed considering various penetration rates. Note that, each diagram corresponds to a particular replication with AVD value closest to the mean AVD value of the respective 10 replications.

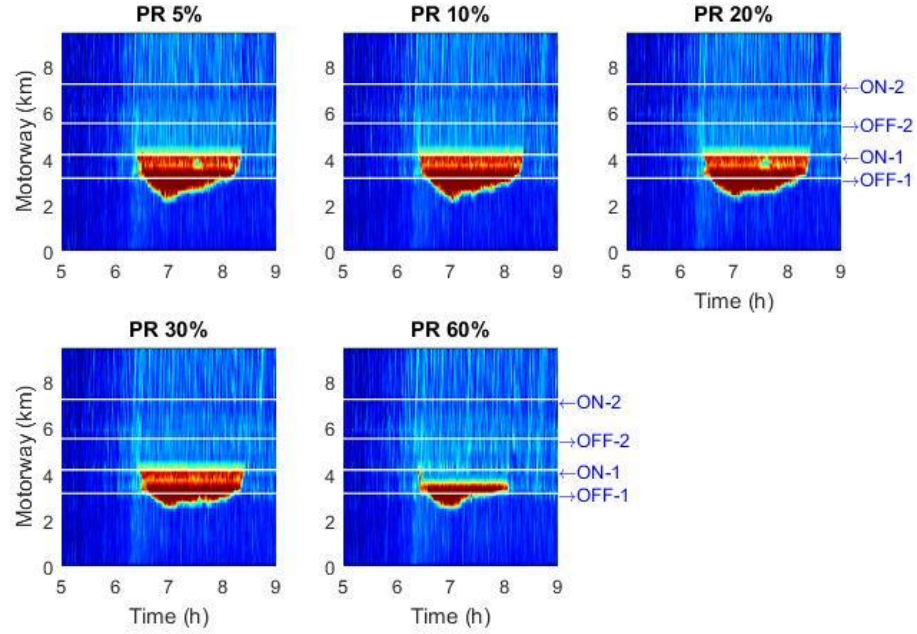


Figure 16 : Traffic Control Case 1: Spatio-temporal diagrams of speed considering various Penetration Rates (PR)

Figure 17 illustrates the spatio-temporal diagrams of the calculated section time-gaps for various penetration rates. It is observed that the time-gap values applied to the vehicles (at the first on-ramp) are decreasing as the penetration rate of the ACC vehicles gets higher. This, in combination with **Figure 16**, suggests that the Traffic Control Case 1 achieves its goal to increase the dynamic and static road capacity but it is not capable to completely dissolve the congestion formatted.

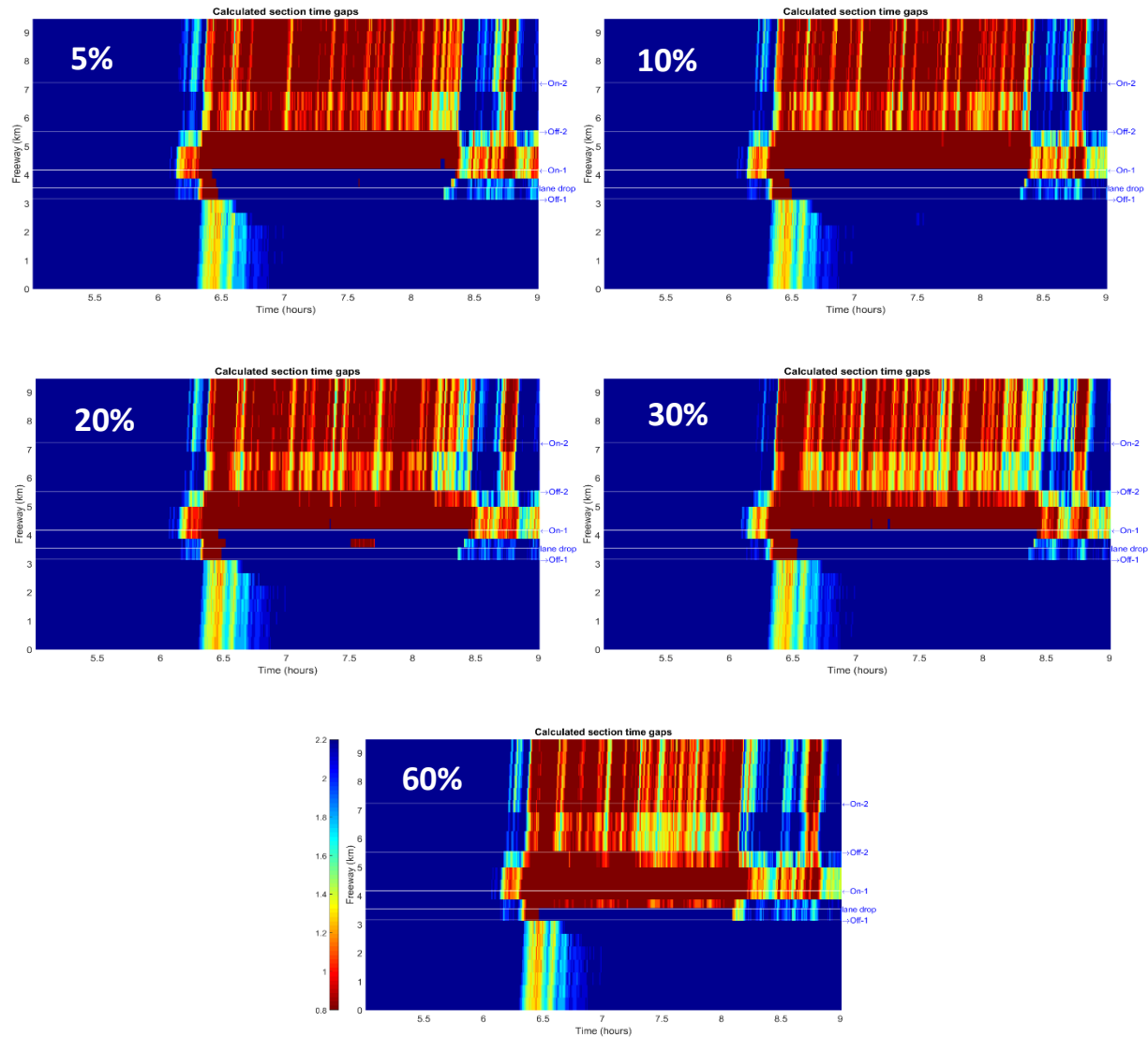


Figure 17 : Traffic Control Case 1: Spatio-temporal diagrams of time-gap considering various Penetration Rates (PR)

Figure 18 displays the trajectories of the outflow from the merge area around the onset of congestion for various penetration rates. The results correspond to the replications with AVD values closest to the mean value of the respective 10 replications just as the spatio-temporal diagrams.

As mentioned at the beginning, the strategy layout stated that the first goal is the increase of the static road capacity by using Equation 1. The following figures are created for the purposes of checking whether the goal mentioned above was achieved.

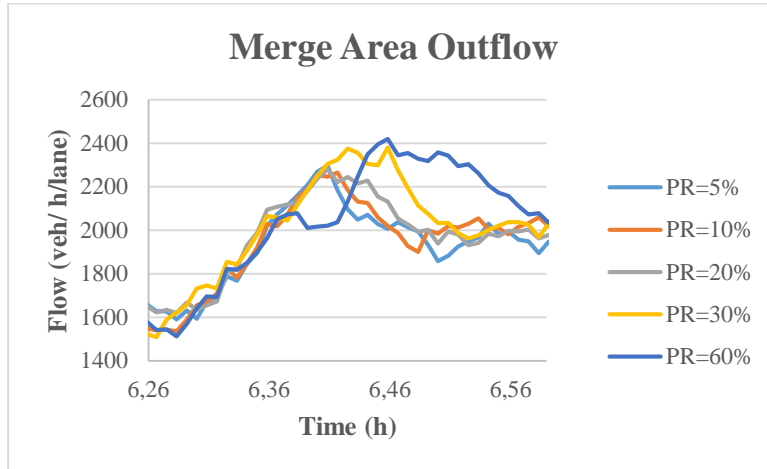


Figure 18 : Time-trajectory of the outflow from the merge (congested) area

From **Figure 18** it can be seen that, for higher penetration rates the onset of congestion is increasingly delayed, as in fact the capacity of the merge area is seen to increase. For example, when the Penetration Rate of the ACC-vehicles is 5% the congestion starts at 6:40 a.m. whereas when the Penetration Rate is 30% the congestion starts later, at about 6:50 a.m.

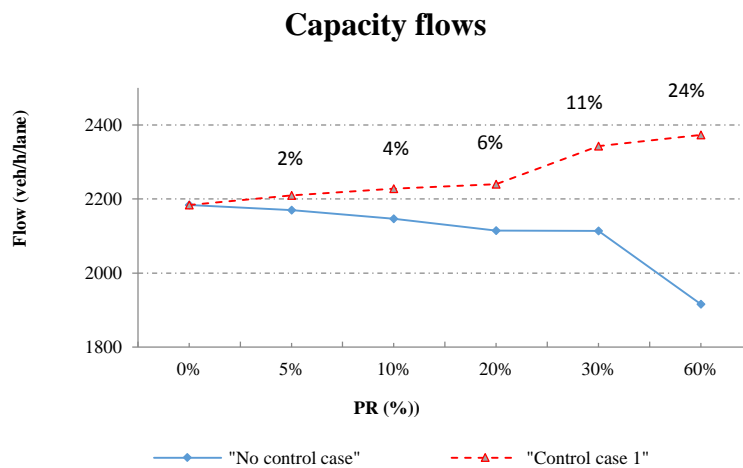


Figure 19 : Capacity flows for No-traffic Control and Control Case 1, for various Penetration Rates

The capacity flows reached at the no-traffic and traffic control case 1 are displayed in **Figure 19** for each corresponding rate. Each point of the graph corresponds to a 5-minute average of flow before breakdown (5 flow values were taken for each Penetration Rate). For the No-Control case we detect that the higher the Penetration Rate, the lower the capacity flow. This occurs due to the bigger time-gaps kept between the vehicles. Whereas, for the Control Case 1 we detect that, the higher the Penetration Rate, the higher the capacity flow so the bigger the achieved improvement. This means that the proposed control strategy achieves its goal and manages to increase the static road capacity.

4.3 Traffic Control Case 2

Traffic control case 2 aims to maximize the discharge flow rate during congestion at the location of active bottlenecks, this depicts the second goal of the proposed strategy overall. In order to achieve that, in addition to Equation 1 we implement only the first part of Equation 2. Specifically, the traffic control case 2 identifies the location of active bottlenecks and sets the suggested time-gap for those sections equal to the minimum time-gap value T_{min} . The parameter Δv which is the threshold speed between two consecutive sections $i - 1$ and i , was set equal to 10 km/h. The settings for the rest of the parameters are the same with the traffic control case 1. It should be noted that, with these parameter settings, the conditions employed in Equation 2 identify the active bottleneck promptly and robustly. The application results of the second part of the control strategy are presented in **Table 4**, in terms of mean AVD and TFC for various penetration rates. Note that, the column Difference (%) states the result change between the No-control case and Control Case 2 for each of the Penetration Rates examined.

Table 4: Control Case 2: Average Vehicle Delay (AVD) and Total Fuel Consumption (TFC) considering various Penetration Rates (PR)

PR	AVD (s/veh/km)			TFC (l)		
	No control	Control case 2	Difference (%)	No control	Control case 2	Difference (%)
0%	19.5	-	-	6786	-	-
5%	21.1	16.0	-24.2	6785	6626	-2.3
10%	21.3	14.9	-29.7	6786	6589	-2.9
20%	24.3	10.5	-56.9	6787	6329	-6.7
30%	27.1	9.5	-64.9	6813	6269	-8.0
60%	44.4	6.4	-85.7	6886	6098	-11.4

It is observed from **Table 4** that the higher the penetration rate, the higher the improvement in mean AVD and TFC. For penetration rate equal to 60% the mean AVD is 6.4 s/veh/km which means that the congestion is resolved and compared to the No-control case the improvement is up to 86% for the corresponding penetration rate. As mentioned above Traffic Control Case 2 constitutes an extension of Traffic Control Case 1, so in order to ascertain whether the second control case is an improvement of the latter a comparison between the results should be made. Comparing Tables 2 and 4 we conclude that the case 2 achieves higher improvement and even

resolves congestion. Note that, the calculated improvements would be even higher for a tighter space-time window around the congestion.

Table 5 : Traffic Control Case 2: Comfort Criteria considering various Penetration Rates (PR)

PR	% ACC cars needed time-gap change	How many times the time-gap changed	How much needed to change (absolute value)	% time of having different time-gap than desired
5%	72.5%	5.5	0.31	54.3%
10%	73.8%	5.8	0.31	53.8%
20%	73.5%	5.9	0.30	52.9%
30%	73.6%	6.0	0.30	52.4%
60%	74.2%	6.4	0.29	53.4%

The comfort criteria for various penetration rates are presented in **Table 5**. Like in Traffic Control Case 1 it is observed that the higher the penetration rate, more frequent and smaller changes need to be done. In this case the 60% penetration rate results do not divert from the general trend.

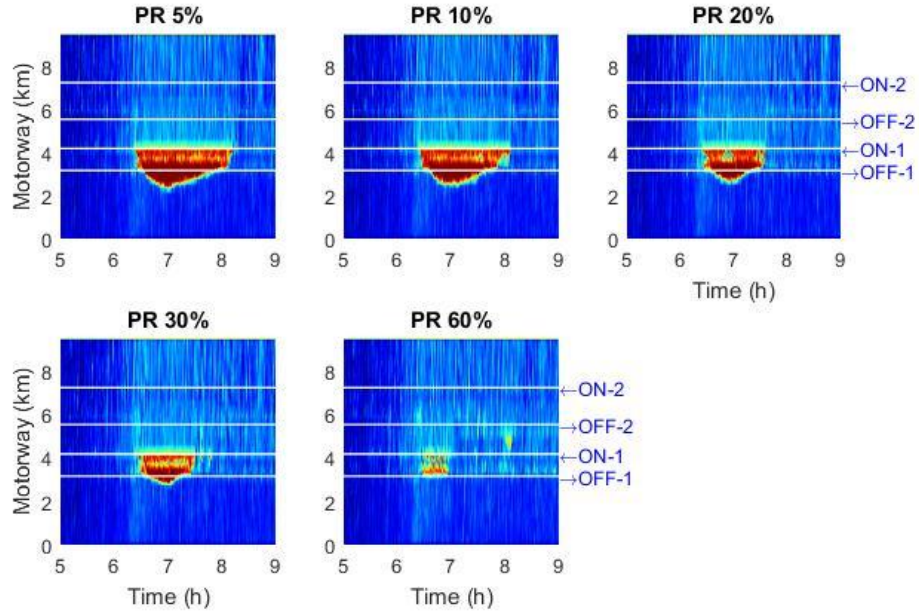


Figure 20 : Traffic Control Case 2: Spatio-Temporal Diagrams of speed considering various Penetration Rates (PR)

Figure 20 presents the Spatio-Temporal diagrams of speed for various penetration rates. We observe that the higher the penetration rate the congestion seems to be minimizing and when the penetration rate is 60% the congestion dissolves. Furthermore, compared to Traffic Control Case 1 (comparison with **Figure 16**), it may be seen that the improvement of traffic conditions is bigger especially for low penetration rates.

Figure 21 illustrates the spatio-temporal diagrams of the calculated section time-gaps for various penetration rates. It is observed that the time-gap values applied to the vehicles, at the first on-ramp, are almost steady and up to 0.8s for all the penetration rates. As the congestion is mitigated, the low time-gap values are gradually increasing at the second off-ramp. For the 60% penetration rate, we can see that between 6:50 and 7:00 the applied time-gap values are 0.8s (the lowest possible) and after that a variation occurs and the applied time-gaps start from 1.2s and sometimes even reach 2.2s.

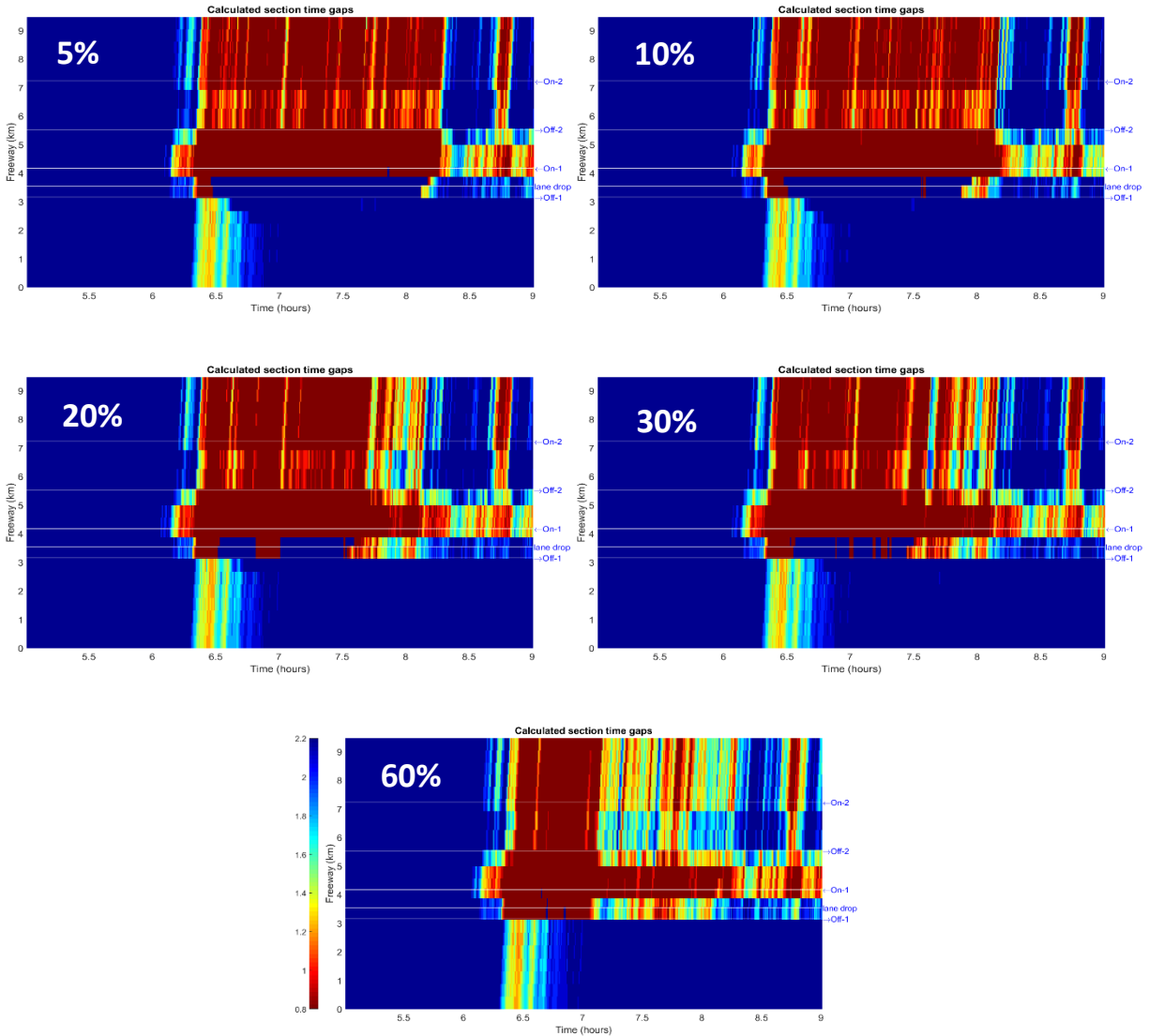


Figure 21 : Traffic Control Case 2: Spatio-Temporal Diagrams of time-gap considering various Penetration Rates (PR)

Combining this figure with **Figure 20** we can conclude that the strategy achieves its goal and at the same time the congestion is dissolved. Moreover, for the 60% case even though the congestion is almost solved the strategy suggests to the drivers the lowest possible time-gap value at the first on-ramp.

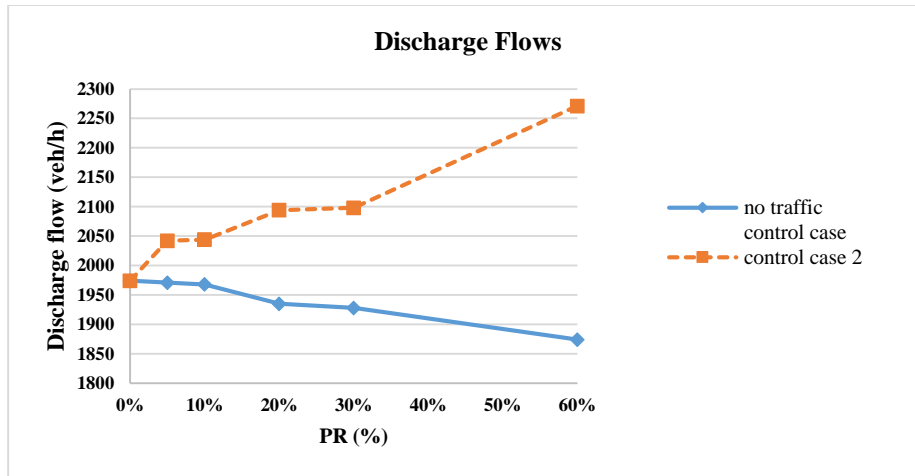


Figure 22 : Capacity flows for No-traffic Control and Control Case 2, for various Penetration Rates

Figure 22 illustrates the average discharge flow during congestion for the no Traffic Control and the Control Case 2 for each corresponding penetration rate. Each point corresponds to a 20 minute average of discharge flow during congestion. It is observed that, in the No-Control Traffic Case the higher the penetration rate of the ACC vehicles, the lower the discharge rate from which the vehicles exit from congestion. While for Control Case 2 the exact opposite happens and the corresponding discharge flows are increased. This means that the higher the penetration rate of ACC vehicles, the higher the discharge flow and the improvement achieved is bigger. As mentioned in the analysis of the results of Traffic Control Case 2 for a penetration rate equal to 60% the congestion on the motorway stretch is almost avoided and the discharge flow is 2271 veh/h whereas for the corresponding No-Control Case the discharge flow is 1870 veh/h.

4.4 Traffic Control Case 3

Traffic control case 3 aims to maximize the discharge flow rate during congestion at the location of active bottlenecks by increasing the acceleration of the ACC vehicles in the bottleneck area. In order to do so, only the second part of equation 2 is used (more precisely Equation 13). Increasing the acceleration of the ACC vehicles at the congestion area, increases the overall outflow out of the congestion head and helps to resolve the congestion after it is formed. The application results

of the Traffic Control Case 3 are presented in **Table 6**, in terms of mean AVD and TFC for various penetration rates. Note that, the column Difference (%) states the result change between the No-control case and Control Case 3 for each of the Penetration Rates examined.

Table 6: Control Case 3: Average Vehicle Delay (AVD) and Total Fuel Consumption (TFC) considering various Penetration Rates (PR)

PR	AVD (s/veh/km)			TFC (l)		
	No control	Control case 3	Difference (%)	No control	Control case 3	Difference (%)
0%	19.5	-	-	6786	-	-
5%	21.1	18.8	-11.4	6785	6725	-0.9
10%	21.3	17.9	-15.8	6786	6663	-1.6
20%	24.3	18.4	-24.3	6787	6617	-2.5
30%	27.1	17.8	-34.4	6813	6555	-3.8
60%	44.4	18.4	-58.5	6886	6494	-7.3

It is observed from **Table 6** that with the increase of the penetration rate of the ACC vehicles the mean AVD remains unchanged and at around 18 s/veh/km. The difference between the No Control Case and the Traffic Control Case 3 for each penetration rate seems to grow bigger due

to the fact that in the No-Control Case the mean AVD as well as the mean TFC seem to worsen and for the Control Case 3 these values remain stable. This shows an important traffic improvement even for low penetration rates.

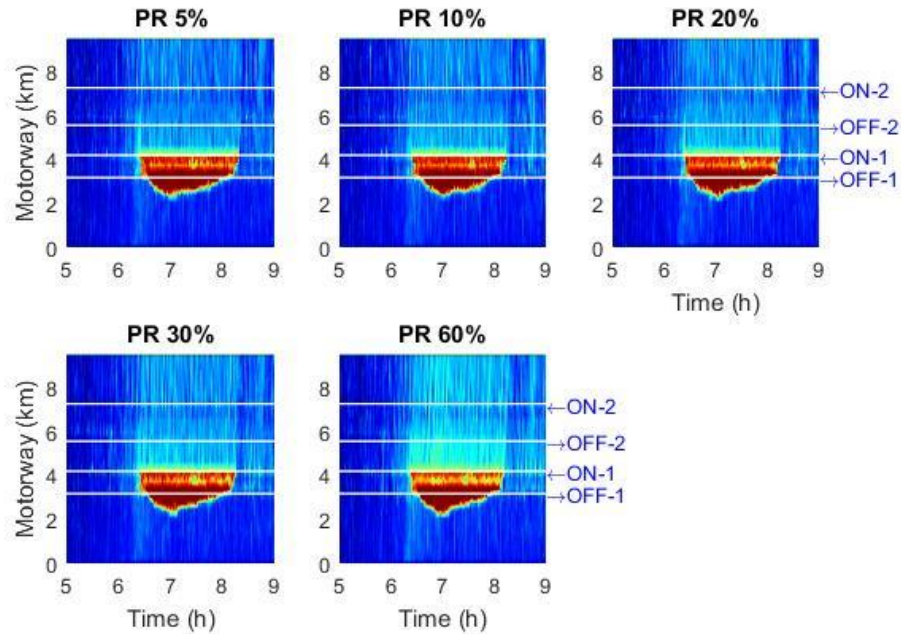


Figure 23 : Traffic Control Case 3: Spatio-temporal diagrams of speed considering various penetration rates (PR)

Figure 23 presents the Spatio-Temporal diagrams of speed for various penetration rates. It is observed that, increasing the acceleration in the bottleneck area for the ACC vehicles, just manages to counterbalance the capacity decrease due to the increased ACC penetration rate with higher time-gaps, with the discharge flow increase due to the increased acceleration in the bottleneck area. Specifically, when examining the spatio-temporal diagram for 60% penetration rate we observe higher speeds near the first on-ramp, as the strategy suggests. Furthermore the speeds achieved after the first on ramp, are the highest from all the penetration rates and confirm the original claim that the maximization of the discharge flow during congestion can also be achieved by increasing the acceleration in bottleneck area.

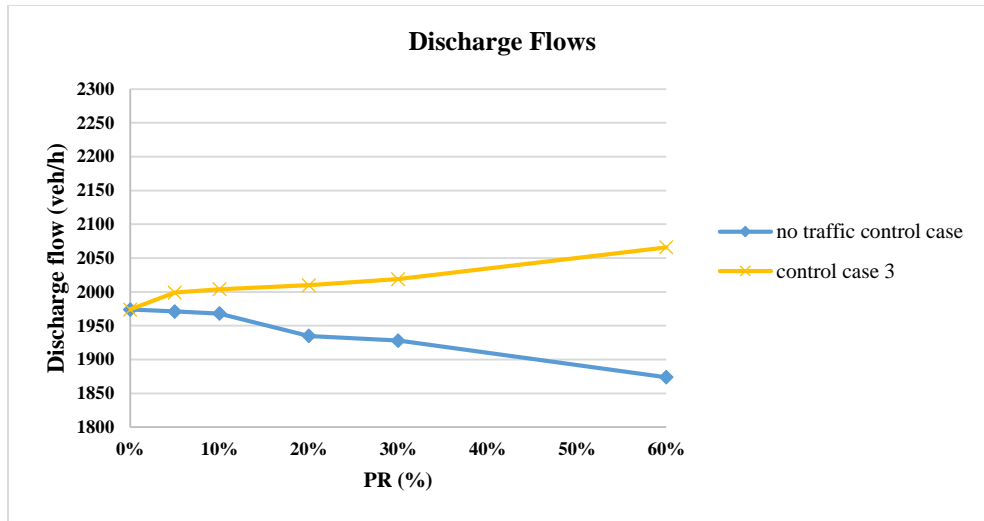


Figure 24 : Capacity flows for No-traffic Control and Control Case 3, for various Penetration Rates

Figure 24 illustrates the average discharge flow during congestion for the no Traffic Control and the Control Case 3 for each corresponding penetration rate. Each point corresponds to a 20 minute average of discharge flow during congestion. It is observed that, in the No-Control Traffic Case the higher the penetration rate of the ACC vehicles, the lower the discharge rate from which the vehicles exit from congestion. While for Control Case 3 the exact opposite happens and the corresponding discharge flows are increased. This means that the higher the penetration rate of ACC vehicles, the higher the discharge flow and the improvement achieved is bigger. However, the achievement improved is significantly lower than the one achieved in Control Case 2. For penetration rate equal to 60% the discharge flow of control case 3 is 2066 veh/h whereas the corresponding value in control case 2 is 2271 veh/h.

4.5 Traffic Control Case 4

Traffic Control Case 4 is a combination between Traffic Control Cases 1 and 3. This means that, the employed equations for this case are Equations 1 and 2. Note that, from Equation 2 only the second part is utilized. Equation 1 is used to increase capacity and from Equation 2 the increased acceleration is used to increase the discharge flow at the active bottleneck area. The application

results of the Traffic Control Case 4 are presented in **Table 7**, in terms of mean AVD and TFC for various penetration rates. Note that, the column Difference (%) states the result change between the No-control case and Control Case 4 for each of the Penetration Rates examined.

Table 7: Control Case 4: Average Vehicle Delay (AVD) and Total Fuel Consumption (TFC) considering various Penetration Rates (PR)

PR	AVD (s/veh/km)			TFC (l)		
	No control	Control case 4	Difference (%)	No control	Control case 4	Difference (%)
0%	19.5	-	-	6786	-	-
5%	21.1	14.7	-30.7	6785	6626	-2.3
10%	21.3	14	-34.4	6786	6528	-3.6
20%	24.3	12.5	-48.4	6787	6461	-4.8
30%	27.1	12.6	-53.5	6813	6469	-5.1
60%	44.4	5.66	-87.2	6886	5914	-14.1

Table 7 shows that the higher the penetration rate of the ACC vehicles for the Control Case 4, the lower the mean AVD values as well as the mean TFC. Furthermore it is detected that the

percentage of the improvement (Column Difference) is comparable with Traffic Control Case 2 where the only difference is the mean we use to increase the discharge flow.

Table 8 : Traffic Control Case 4: Comfort Criteria considering various Penetration Rates (PR)

PR	% ACC cars needed time-gap change	How many times the time-gap changed	How much needed to change (absolute value)	% time of having different time-gap than desired
5%	73.3%	5.8	0.30	49.5%
10%	73.5%	6.1	0.29	48.6%
20%	73.4%	6.3	0.28	48.1%
30%	74.0%	6.7	0.28	48.7%
60%	72.7%	6.4	0.28	43.9%

The comfort criteria for various penetration rates are presented in **Table 8**. This case combines both the time-gap and the acceleration equations. We observe that the higher the penetration rate, more changes to the time-gap need to be done. From all replications a mean of 73% of the ACC vehicles needed time-gap change with the lower percentage occurring at 60%. Also for this penetration rate we have the lowest percentage of time the drivers had different time-gap than the desired.

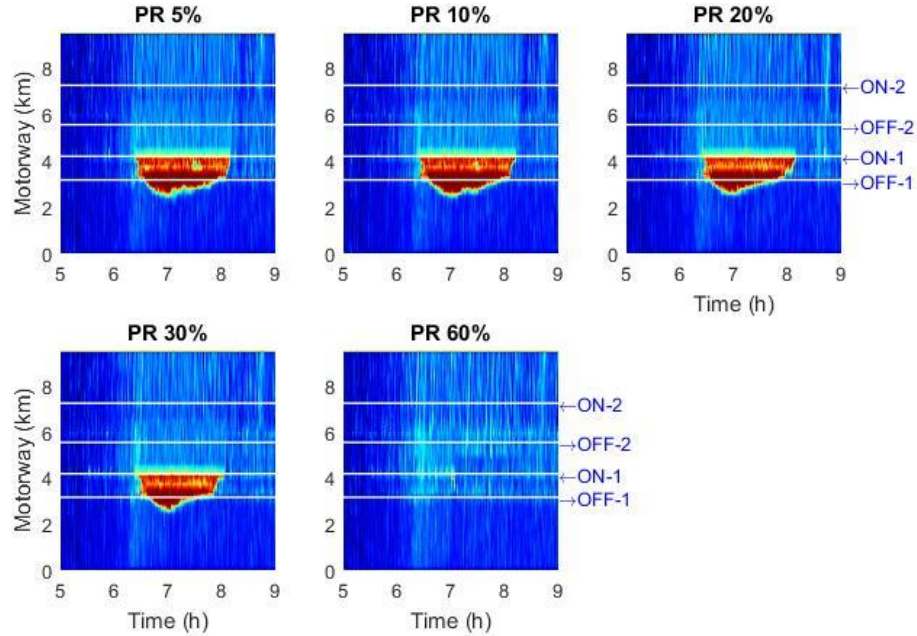


Figure 25 : Traffic Control Case 4: Spatio-temporal diagrams of speed considering various Penetration Rates (PR)

Figure 25 illustrates the spatio-temporal diagrams of speed considering various penetrations rates. As mentioned above the results of this case are similar to the ones from Control Case 2 and like Case 2, when the penetration rate of ACC vehicles is 60%, the congestion on the motorway stretch is fully avoided. In detail, for this penetration rate an improvement of 87.2% for the mean AVD and 14.1% for the mean TFC is observed compared to the No Traffic Control Case. Even for lower penetration rates important improvement is achieved.

Figure 26 illustrates the spatio-temporal diagrams of the calculated section time-gaps for various penetration rates. It is observed that the time-gap values applied to the vehicles, at the first on-ramp, are almost steady and up to 0.8s for all the penetration rates. As the congestion is mitigated, the low time-gap values are gradually increasing at the second off-ramp. For the 60% penetration rate, we can see that between 6:50 and 7:00 the applied time-gap values are 0.8s (the lowest possible) and after that a variation occurs and the applied time-gaps start from 1.2s and sometimes even reach 2.2s.

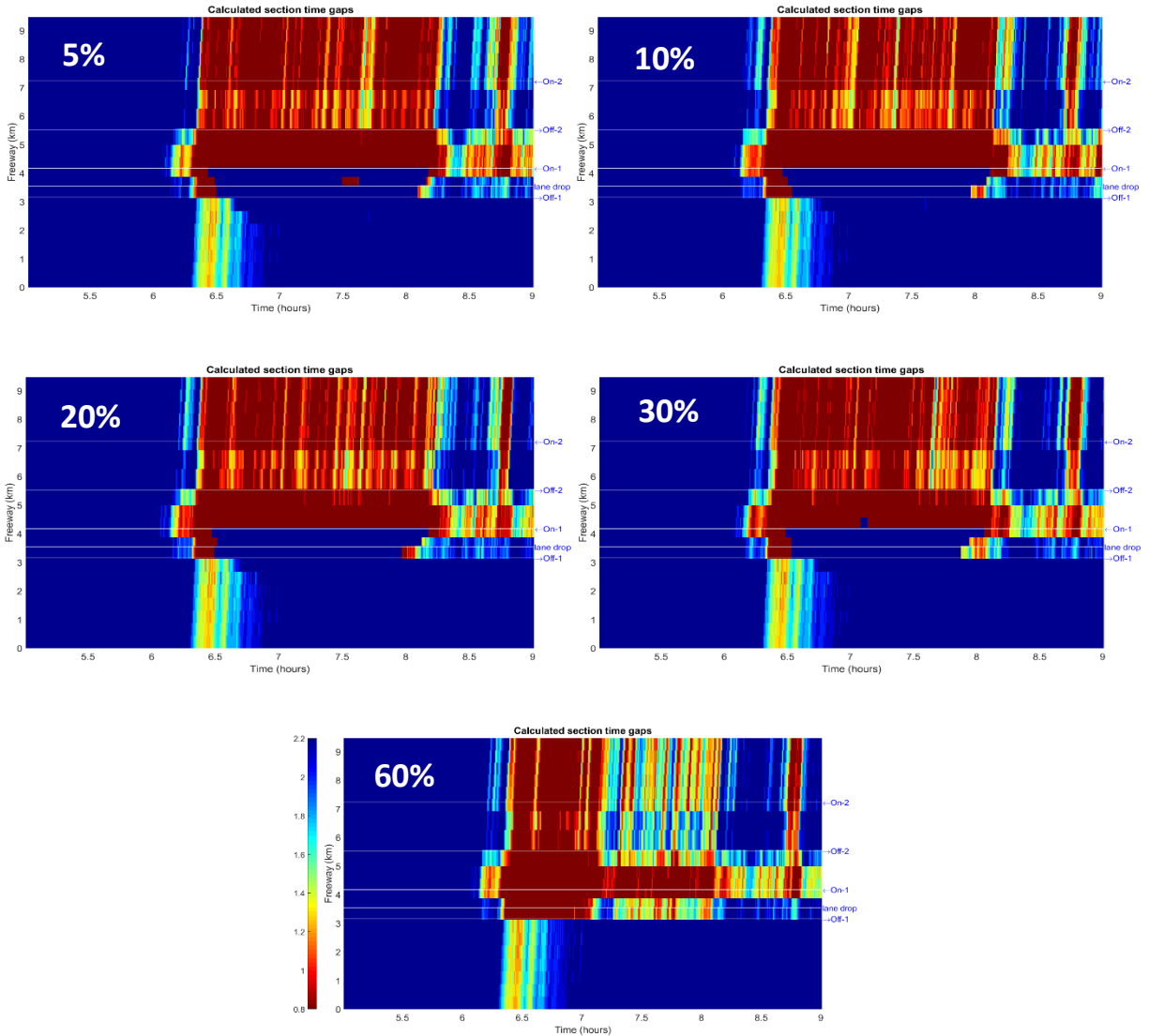


Figure 26 : Traffic Control Case 4: Spatio-temporal diagrams of time-gap considering various Penetration Rates (PR)

Combining this figure with **Figure 25** we can conclude that the strategy achieves its goal and at the same time the congestion is dissolved. Moreover, for the 60% case even though the congestion is almost solved the strategy suggests to the drivers the lowest possible time-gap value at the first on-ramp.

This diagram is similar to **Figure 21** from Traffic Control Case 2 where the congestion is also dissolved.

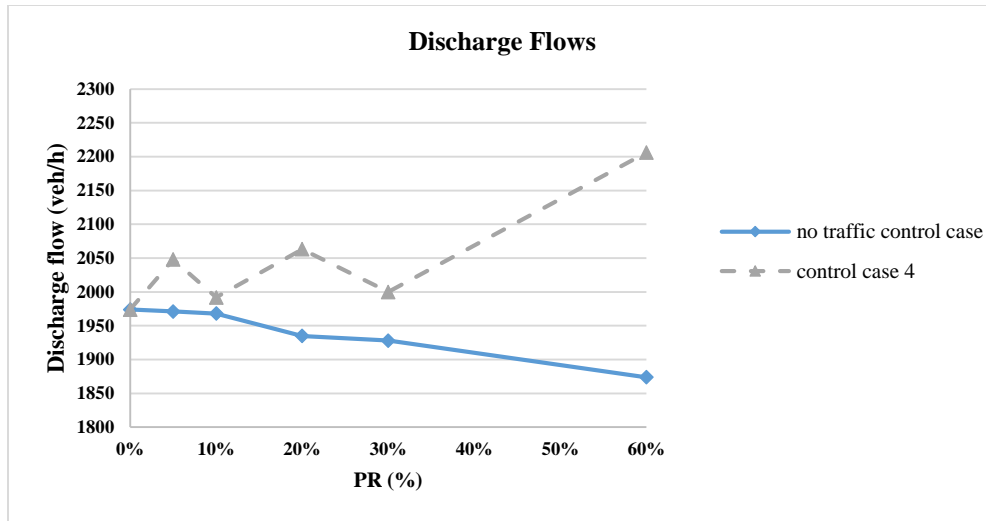


Figure 27 : Capacity flows for No-traffic Control and Control Case 4, for various Penetration Rates

Figure 27 illustrates the average discharge flow during congestion for the No Traffic Control and the Control Case 4 for each corresponding penetration rate. Control Case 4 seems to have inconsistencies concerning the discharge flow. These inconsistencies occur due to the fact that the penetration rate of ACC vehicles affects the discharge flow of the bottleneck both positively and negatively (like Control Case 3) depending the situation. In spite of the unconformities, in **Figure 27** a significant discharge flow increase can be seen in comparison with the No Traffic Control Case for all penetration rates. Even when the penetration rate is 10% the discharge flow is 1968 veh/h for the No Control Case, whereas for Case 4 the corresponding value is 1992 veh/h.

4.6 Traffic Control Case 5

Traffic Control Case 5 is the full control case. This means that the equations employed simultaneously are Equation 1 plus the two components of Equation 2. In particular, this strategy aims to increase the discharge flow at the active bottleneck area by identifying that area then setting the minimum time-gap T_{min} and by increasing the acceleration in all vehicles located in the sections just before and just after the congestion head. The expectation is to observe a very quick resolution of the congestion if there is one. The application results of the full control case are presented in **Table 9**, in terms of mean AVD and TFC for various penetration rates. Note

that, the column Difference (%) states the result change between the No-control case and Control Case 4 for each of the Penetration Rates examined.

Table 9: Control Case 5: Average Vehicle Delay (AVD) and Total Fuel Consumption (TFC) considering various Penetration Rates (PR)

PR	AVD (s/veh/km)			TFC (l)		
	No control	Control case 5	Difference (%)	No control	Control case 5	Difference (%)
0%	19.5	-	-	6786	-	-
5%	21.1	11.7	-44.8	6785	6626	-2.3
10%	21.3	9.1	-57.1	6786	6267	-1.5
20%	24.3	8.1	-66.8	6787	6185	-8.9
30%	27.1	7.5	-72.4	6813	6187	-9.2
60%	44.4	5.0	-88.8	6886	5985	-13.1

Table 9 shows for Traffic Control Case 5 the improvement on the network which is significant even for the lower penetration rates and consistent. When the penetration rate of the ACC vehicles is 60% there is no congestion as it is shown that the mean AVD is 5 s/veh/km. This

occurs due to the greatest possible increase of the discharge flow, as illustrated in **Figure 28**, which leads to the quick resolution of the congestion.

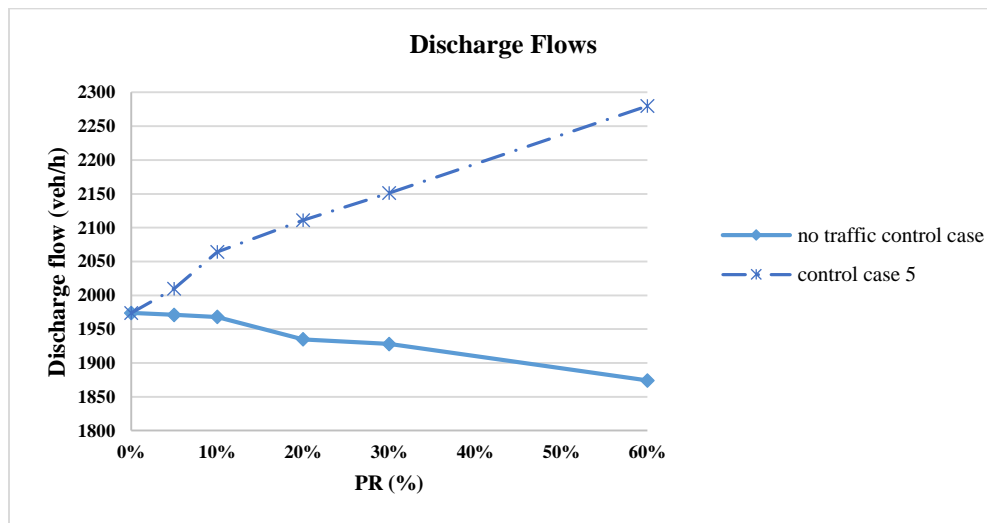


Figure 28 : Discharge flows for the No-Traffic Control and Complete Traffic Control Case, for various Penetration Rates (PR)

Table 10 : Traffic Control Case 5: Comfort Criteria considering various Penetration Rates (PR)

PR	% ACC cars needed time-gap change	How many times the time-gap changed	How much needed to change (absolute value)	% time of having different time-gap than desired
5%	71.7%	5.5	0.31	53.3%
10%	73.2%	5.9	0.30	51.7%
20%	72.6%	6.0	0.30	49.4%
30%	72.6%	6.0	0.31	52.0%
60%	72.8%	6.3	0.28	44.1%

Table 10 illustrates the comfort criteria for Traffic Control Case 5 (full Control Case) considering various Penetration Rates. The percentage of vehicles that needed time-gap change are steady for all the penetration rates, whereas the times the time-gap changed is inversely proportional to the absolute value the time-gap needed to change. In spite of the above, it can also be observed that the percentage of time the vehicles had different time-gap from the desired for the case of 60% is the lowest possible for this control strategy. We can conclude that even though the same percentage of cars needs to change their time-gap in the full control case, the changes applied are smaller and more frequent. Note that in 60% the congestion is completely dissolved.

Figure 29 illustrates the spatio-temporal diagrams of speed considering various penetrations rates. From these diagrams we confirm our original assumption that the congestion, when it occurs, is rapidly dissolved. Also, the spatio-temporal diagram of speed for penetration rate 60% shows no congestion formed.

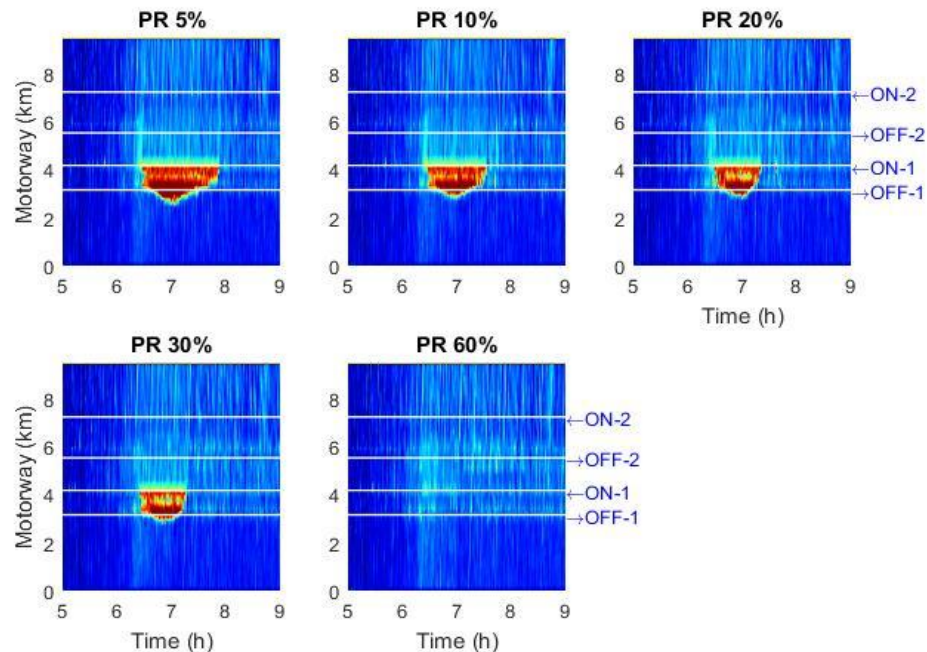


Figure 29 : Traffic Control Case 5 (Full Control Case): Spatio-temporal diagrams of speed considering various Penetration Rates (PR)

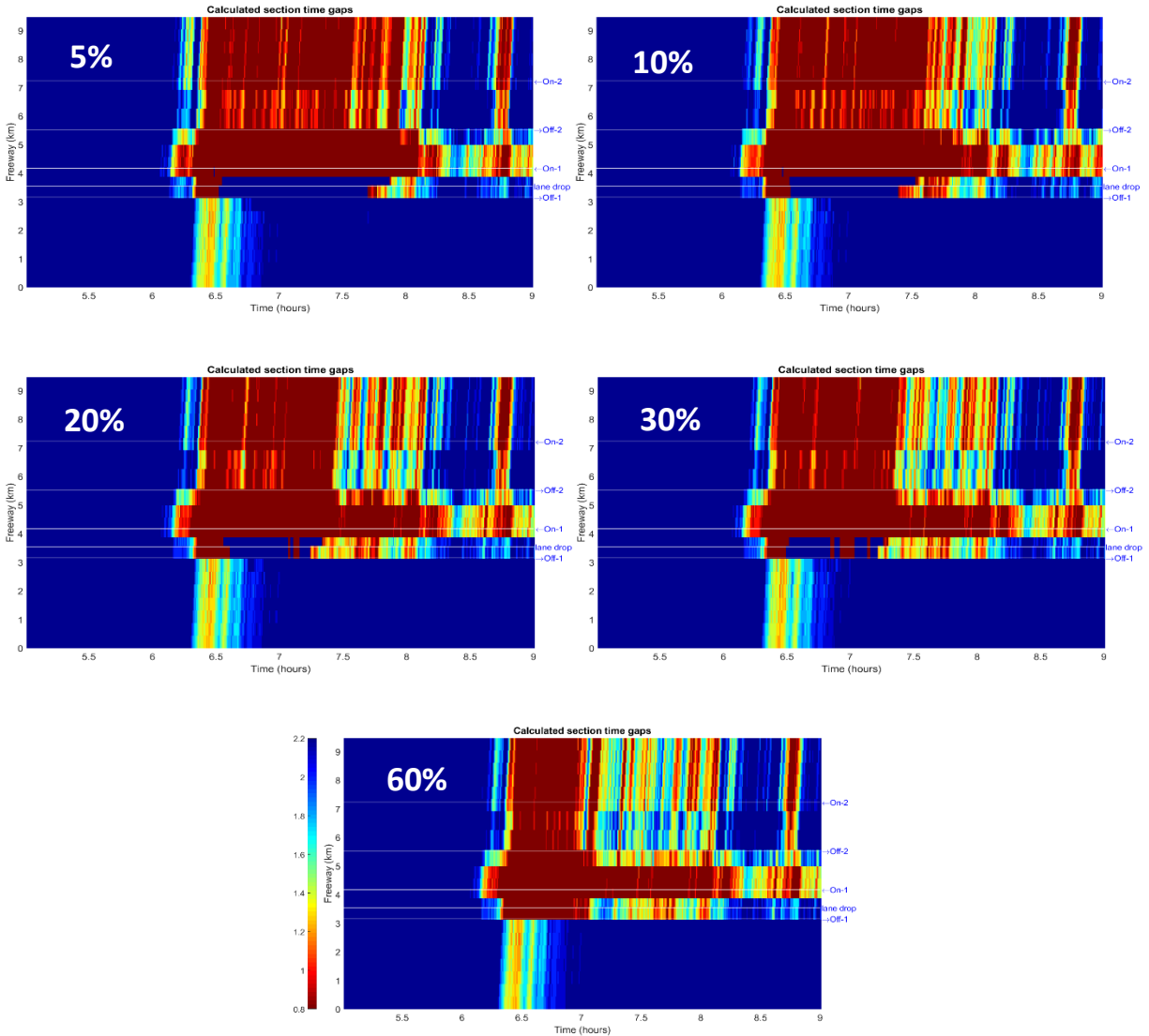


Figure 30 : Traffic Control Case 5 (Full Control Case): Spatio-temporal diagrams of time-gap considering various Penetration Rates (PR)

Figure 30 illustrates the spatio-temporal diagrams of the calculated section time-gaps for various penetration rates. It is observed that the time-gap values applied to the vehicles, at the first on-ramp, are almost steady and up to 0.8s for all the penetration rates. As the congestion is mitigated, the low time-gap values are gradually increasing at the second off-ramp. For the 60% penetration rate, we can see that between 6:50 and 7:00 the applied time-gap values are 0.8s (the lowest possible) and after that a variation occurs and the applied time-gaps start from 1.2s and sometimes even reach 2.2s. This diagram is similar to **Figure 21** from Traffic Control Case 2 and **Figure 26** from Traffic Control Case 4 where the congestion is also dissolved.

Combining this figure with **Figure 25** we can conclude that the strategy achieves its goal and at the same time the congestion is dissolved. Moreover, for the 60% case even though the congestion is almost solved the strategy suggests to the drivers the lowest possible time-gap value at the first on-ramp. The main difference with the previous cases is that the congestion is solved faster and as a result the time-gap values after the first on-ramp are higher (due to the fact that there is no congestion and the speeds are higher).

4.7 Traffic Control Cases Summary

In this section we will summarize all the examined control cases presented. Firstly, **Table 11** shows for each of the control cases the scenarios used as well as the equations which support them.

The equations mentioned above have a distinct role for each part of the proposed control strategy.

Equation 1 is used to increase the static capacity at bottleneck locations where the level of increase depends on the penetration rate of the ACC vehicles. If the achievable capacity increase is sufficient to accommodate the arriving demand, then the activation of the bottleneck may be avoided altogether. For the cases examined, this happens mostly when the penetration rate is 60%. For the rest of the cases, when the arriving demand is higher than the increased capacity, congestion is formed which can merely be delayed. This leads to a reduction of the congestion extent as well as to the corresponding traffic improvements. However, Equation 1 remains essentially inactive after the onset of congestion.

Equation 2 is applied only if congestion actually forms, else the conditions stated on chapter 3 are not satisfied and this part of the control strategy remains inactive. However, if congestion is actually formed then this part of the strategy is employed. Due to the increase of the discharge flow we achieve faster resolution of the congestion with corresponding benefits for the traffic flow efficiency. This shows the significant contribution equation 2 has to the proposed control strategy. This equation consists of two independent components which can either be used separately or together. The first is the minimization of the ACC vehicles time-gap in case of

active bottleneck and the second is to increase the ACC vehicles' acceleration until a safe maximum acceleration is reached.

Table 11: Traffic Control Cases

Control Cases	Scenarios	Time gap equation 1	Time gap equation 2	Acceleration equation 2
No Traffic Control Case	-	-	-	-
Control Case 1	Set the appropriate time-gap (bottleneck area T_{max})	x	-	-
Control Case 2	Set the appropriate time-gap (bottleneck area T_{min})	x	x	-
Control Case 3	Increase acceleration in bottleneck area	-	-	x
Control Case 4	Case 1 + Case 3	x	-	x
Control Case 5	Case 2 + Case 3	x	x	x

Table 12 : No-Traffic Control and Control Cases: Average Vehicle Delay (AVD) and Total Fuel Consumption (TFC) considering various Penetration Rates (PR)

Performance Indices		Penetration Rates (PR)					
		0%	5%	10%	20%	30%	60%
AVD (s/veh/km)	No-Traffic Control	19.5	21.1	21.3	24.3	27.1	44.4
	Control Case 1	-	18.7	18.5	17.7	15.9	12.0
	Control Case 2	-	16.0	14.9	10.5	9.5	6.4
	Control Case 3	-	18.8	17.9	18.4	17.8	18.4
	Control Case 4	-	14.7	14	12.5	12.6	5.66
	Control Case 5 (Complete Control Case)	-	11.7	9.1	8.1	7.5	5.0
TFC (l)	No-Traffic Control	6786	6785	6786	6787	6813	6886
	Control Case 1	-	6742	6685	6619	6487	6317
	Control Case 2	-	6626	6589	6329	6269	6098
	Control Case 3	-	6725	6663	6617	6555	6494
	Control Case 4	-	6626	6528	6461	6469	5914
	Control Case 5 (Complete Control Case)	-	6626	6267	6185	6187	5985

The summarization of all the Control Cases results as well as the No-Traffic Control Case, are shown in **Table 12**. From this table, it is shown that as we enrich the control strategy, the network traffic conditions improve. This also can be seen from **Figure 31** which illustrates the discharge flows for all the Traffic Control Cases tested as well as the No Traffic Control Case.

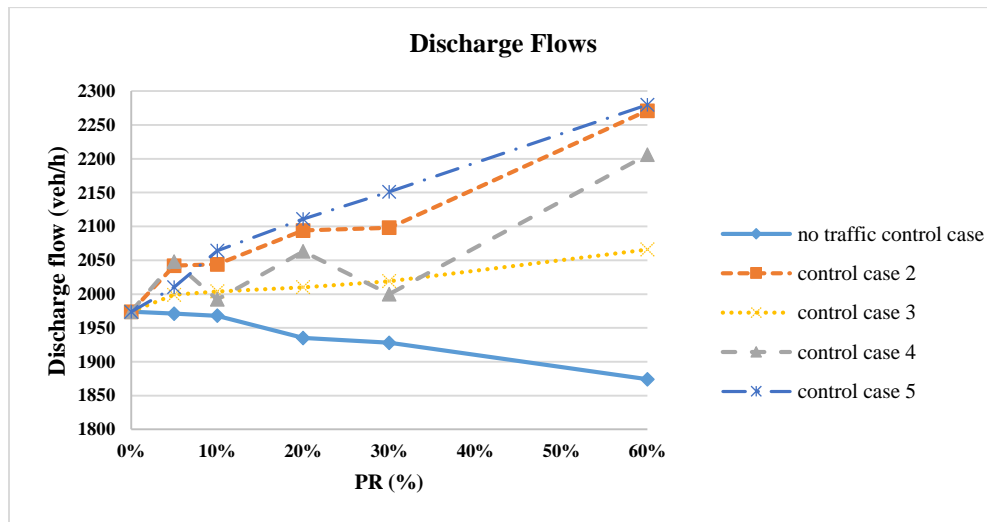


Figure 31 : Discharge flows for the No-Traffic Control and all Traffic Control Cases, for various Penetration Rates (PR)

Table 13 : Traffic Control Cases: Comfort Criteria considering various Penetration Rates (PR)

Performance Indices		Penetration Rates				
		5%	10%	20%	30%	60%
How many times the time-gap changed	Control Case1	6.1	6.7	7.0	7.2	7.2
	Control Case 2	5.5	5.8	5.9	6.0	6.4
	Control Case 4	5.8	6.1	6.3	6.7	6.4
	Control Case 5 (Complete Control Case)	5.5	5.9	6.0	6.0	6.3
How much needed to change (absolute value)	Control Case1	0.30	0.28	0.27	0.26	0.26
	Control Case 2	0.31	0.31	0.30	0.30	0.29
	Control Case 4	0.30	0.29	0.28	0.28	0.28
	Control Case 5 (Complete Control Case)	0.31	0.30	0.30	0.31	0.28

Finally, **Table 13** shows the comfort criteria of the time-gap changes. We can see that increasing the penetration rate of the ACC vehicles, leads to more but lower changes of the implemented time-gaps.

5. Conclusions and Future Work

5.1 Thesis Summary

The objective of this thesis was the creation of a simple and effective ACC-based control strategy, which aimed to dynamically adapt the driving behavior of ACC-equipped vehicles so that the motorway traffic flow efficiency would be improved. The proposed strategy was tested using the microscopic traffic simulator AIMSUN using a real traffic motorway (Motorway A20 in The Netherlands) stretch where congestion is created due to an on-ramp bottleneck. The simulation results demonstrate that for various, even low, penetration rates of ACC-vehicles, the proposed control concept improves the traffic conditions in general. Specifically, the average vehicle delay and the total fuel consumption have lower values compared to the case of only manually-driven or regular ACC-vehicles. This improvement is achieved by retarding the onset and reducing the space-time extent of the congestion in comparison to the no control case. IDM has been used for both manual and ACC vehicles to ensure that the results would reflect the time-gap effects to the traffic. Microscopic simulation is useful in this sort of investigations, but, due to several uncertainties regarding the dynamics of ACC vehicles, the produced simulation-based traffic level comparisons and improvements might turn out to be quantitatively different if the proposed concept would be applied in real conditions. However, the obtained results are useful to demonstrate and evaluate the impact tendency and pertinence of the concept.

5.2 Conclusions

The conclusions that derive from the ACC-based control strategy which was created in order to improve the traffic flow on motorways are:

- The IDM cannot accurately depict the behavior of the ACC vehicles because of the different dynamics between manual and ACC vehicles.
- The strategy solves (or mitigates) the congestion.
- The strategy manages to increase the discharge flow as well as to increase the capacity in the merge area, even for lower penetration rates of ACC vehicles (i.e. 5%).

5.3 Future Work

In this research work, only the dynamic adaptation of the time-gap settings was considered. Future work should be testing alternative car following models for ACC vehicles, in a way that the results would be affected not only by the ACC parameters, but also by the different dynamics between manual and ACC vehicles.

References

- [1] J. VanderWerf, S. Shladover, N. Kourjanskaia, M. Miller, and H. Krishnan, "Modeling Effects of Driver Control Assistance Systems on Traffic," *Transp. Res. Rec. J. Transp. Res. Board*, 2001.
- [2] A. Bose and P. A. Ioannou, "Analysis of traffic flow with mixed manual and semiautomated vehicles," *IEEE Trans. Intell. Transp. Syst.*, 2003.
- [3] L. C. Davis, "Effect of adaptive cruise control systems on traffic flow," *Phys. Rev. E - Stat. Nonlinear, Soft Matter Phys.*, 2004.
- [4] P. A. Ioannou and M. Stefanovic, "Evaluation of ACC vehicles in mixed traffic: Lane change effects and sensitivity analysis," in *IEEE Transactions on Intelligent Transportation Systems*, 2005.
- [5] B. Van Arem, C. J. G. Van Driel, and R. Visser, "The impact of cooperative adaptive cruise control on traffic-flow characteristics," *IEEE Trans. Intell. Transp. Syst.*, 2006.
- [6] W. J. Schakel, B. Van Arem, and B. D. Netten, "Effects of Cooperative Adaptive Cruise Control on Traffic Flow Stability," *Intell. Transp. Syst. (ITSC), 2010 13th Int. IEEE Conf.*, 2010.
- [7] G. Arnaout and S. Bowling, "Towards reducing traffic congestion using cooperative adaptive cruise control on a freeway with a ramp," *J. Ind. Eng. Manag.*, 2011.
- [8] S. Shladover, D. Su, and X.-Y. Lu, "Impacts of Cooperative Adaptive Cruise Control on Freeway Traffic Flow," *Transp. Res. Rec. J. Transp. Res. Board*, 2012.
- [9] I. A. Ntousakis, I. K. Nikolos, and M. Papageorgiou, "On Microscopic Modelling of Adaptive Cruise Control Systems," in *Transportation Research Procedia*, 2015.
- [10] B. Bayar, S. A. Sajadi-Alamdari, F. Viti, and H. Voos, "Impact of different spacing policies for adaptive cruise control on traffic and energy consumption of electric vehicles," in *24th Mediterranean Conference on Control and Automation, MED 2016*, 2016.
- [11] D. Ngoduy, S. P. Hoogendoorn, and R. Liu, "Continuum modeling of cooperative traffic flow dynamics," *Phys. A Stat. Mech. its Appl.*, 2009.
- [12] D. Ngoduy, "Application of gas-kinetic theory to modelling mixed traffic of manual and ACC vehicles," *Transportmetrica*, 2012.
- [13] D. Ngoduy, "Instability of cooperative adaptive cruise control traffic flow: A macroscopic

- approach,” *Commun. Nonlinear Sci. Numer. Simul.*, 2013.
- [14] I. K. Nikolos, A. I. Delis, and M. Papageorgiou, “Macroscopic Modelling and Simulation of ACC and CACC Traffic,” in *IEEE Conference on Intelligent Transportation Systems, Proceedings, ITSC*, 2015.
- [15] A. I. Delis, I. K. Nikolos, and M. Papageorgiou, “Simulation of the penetration rate effects of ACC and CACC on macroscopic traffic dynamics,” in *IEEE Conference on Intelligent Transportation Systems, Proceedings, ITSC*, 2016.
- [16] C. U. Mba and C. Novara, “Evaluation and optimization of Adaptive Cruise Control policies via numerical simulations,” in *VEHITS 2016 - 2nd International Conference on Vehicle Technology and Intelligent Transport Systems, Proceedings*, 2016.
- [17] H. Liu, H. Wei, T. Zuo, Z. Li, and Y. J. Yang, “Fine-tuning ADAS algorithm parameters for optimizing traffic safety and mobility in connected vehicle environment,” *Transp. Res. Part C Emerg. Technol.*, 2017.
- [18] W. J. Schakel, G. Klunder, B. van Arem, E. Harmsen, and M. P. Hagenzieker, “Reducing travel delay by in-car advice on speed, headway and lane use based on downstream traffic flow conditions - a simulation study,” *Proc. 15th Meet. Euro Work. Gr. Transp. EWGT 2012, Paris (France), 10-13 Sept. 2012*, 2012.
- [19] W. J. Schakel and B. Van Arem, “Improving traffic flow efficiency by in-car advice on lane, speed, and Headway,” *IEEE Trans. Intell. Transp. Syst.*, 2014.
- [20] A. Kesting, M. Treiber, M. Schönhof, and D. Helbing, “Adaptive cruise control design for active congestion avoidance,” *Transp. Res. Part C Emerg. Technol.*, 2008.
- [21] A. Kesting, M. Treiber, and D. Helbing, “Enhanced intelligent driver model to access the impact of driving strategies on traffic capacity,” *Philos. Trans. R. Soc. A Math. Phys. Eng. Sci.*, 2010.
- [22] “ISO 15622:2010 - Intelligent transport systems -- Adaptive cruise control systems -- Performance requirements and test procedures,” 2010.
- [23] N. Bekiaris-Liberis, C. Roncoli, and M. Papageorgiou, “Highway traffic state estimation with mixed connected and conventional vehicles,” *IEEE Trans. Intell. Transp. Syst.*, 2016.
- [24] A. Spiliopoulou, D. Manolis, F. Vadorou, and M. Papageorgiou, “Adaptive Cruise Control Operation for Improved Motorway Traffic Flow,” *97th Annu. Meet. Transp. Res. Board Compend.*

- Pap.*, vol. 2250, p. 036119811879602, Sep. 2018.
- [25] *Aimsun User's Manual v8*. 2014.
- [26] *Aimsun Dynamic Simulators Manual v8*. 2014.
- [27] G. Perraki, "Evaluation of a model predictive control strategy on a calibrated multilane microscopic model," Technical University of Crete, 2016.
- [28] G. Perraki, C. Roncoli, I. Papamichail, and M. Papageorgiou, "Evaluation of an MPC strategy for motorway traffic comprising connected and automated vehicles," in *IEEE Conference on Intelligent Transportation Systems, Proceedings, ITSC*, 2018.
- [29] M. Treiber, A. Hennecke, and D. Helbing, "Congested traffic states in empirical observations and microscopic simulations," *Phys. Rev. E - Stat. Physics, Plasmas, Fluids, Relat. Interdiscip. Top.*, 2000.
- [30] V. Milanés and S. E. Shladover, "Modeling cooperative and autonomous adaptive cruise control dynamic responses using experimental data," *Transp. Res. Part C Emerg. Technol.*, 2014.
- [31] C. Nowakowski *et al.*, "Cooperative Adaptive Cruise Control: Testing Drivers' Choices of Following Distances," 2011.